Published for SISSA by Springer

Received: November 22, 2018
Revised: January 4, 2019
Accepted: February 21, 2019
Published: March 5, 2019

Self-interacting dark matter with a vector mediator: kinetic mixing with the U(1)$_{(B-L)_3}$ gauge boson

Ayuki Kamada,[a] **Masaki Yamada**[b] **and Tsutomu T. Yanagida**[c,d,1]

[a] *Center for Theoretical Physics of the Universe, Institute for Basic Science (IBS), 55 Expo-ro, Yuseong-gu, Daejeon 34126, Korea*

[b] *Institute of Cosmology, Department of Physics and Astronomy, Tufts University, 574 Boston Avenue, Medford, MA 02155, U.S.A.*

[c] *Kavli IPMU (WPI), UTIAS, The University of Tokyo, 5-1-5 Kashiwanoha, Kashiwa, Chiba 277-8583, Japan*

[d] *T.D. Lee Institute and School of Physics and Astronomy, Shanghai Jiao Tong University, 800 Dongchuan Rd, Shanghai 200240, China*

E-mail: akamada@ibs.re.kr, Masaki.Yamada@tufts.edu, tsutomu.tyanagida@ipmu.jp

Abstract: A spontaneously broken hidden U(1)$_h$ gauge symmetry can explain both the dark matter stability and the observed relic abundance. In this framework, the light gauge boson can mediate the strong dark matter self-interaction, which addresses astrophysical observations that are hard to explain in collisionless cold dark matter. Motivated by flavoured grand unified theories, we introduce right-handed neutrinos and a flavoured $B-L$ gauge symmetry for the third family U(1)$_{(B-L)_3}$. The unwanted relic of the U(1)$_h$ gauge boson decays into neutrinos via the kinetic mixing with the U(1)$_{(B-L)_3}$ gauge boson. Indirect detection bounds on dark matter are systematically weakened, since dark matter annihilation results in neutrinos. However, the kinetic mixing between U(1)$_{(B-L)_3}$ and U(1)$_Y$ gauge bosons are induced by quantum corrections and leads to an observable signal in direct and indirect detection experiments of dark matter. This model can also explain the baryon asymmetry of the Universe via the thermal leptogenesis. In addition, we discuss the possibility of explaining the lepton flavour universality violation in semi-leptonic B meson decays that is recently found in the LHCb experiment.

Keywords: Cosmology of Theories beyond the SM, Beyond Standard Model

ArXiv ePrint: 1811.02567

[1] Hamamatsu Professor.

https://doi.org/10.1007/JHEP03(2019)021

Contents

JHEP03(2019)021

1 Introduction

The nature of dark matter (DM) is a longstanding mystery in cosmology and particle physics. If DM consists of some new particle, it needs to be long-lived and its relic density should explain the observed amount. A simple framework to explain these aspects is to introduce a gauge symmetry $\mathrm{U}(1)_h$, which is broken to some discrete group. The DM particle is stable due to the unbroken discrete group and the correct relic density is obtained through the DM annihilation into light gauge bosons Z_h.

The light gauge boson mediates a DM self-interaction, which can address small-scale issues in structure formation of collisionless cold dark matter (see, e.g., refs. [1, 2]). The self-interaction is velocity-dependent as astrophysical observations prefer [3]. The cross section per mass is $\sigma/m \gtrsim 1\,\mathrm{cm}^2/\mathrm{g}$ in (dwarf) galaxies to explain, e.g., diversity in galaxy

rotation curves [4–6] (see also ref. [7]). Meanwhile it diminishes to $\sigma/m \lesssim 0.1\,\mathrm{cm}^2/\mathrm{g}$ in galaxy clusters to be compatible, e.g., with the inferred core of relaxed galaxy clusters [3] (see also ref. [8]). The circular velocity in galaxy clusters is of order $v \sim 1000\,\mathrm{km/s}$, while that in dwarf galaxies is of order $v \sim 30\mathrm{km/s}$. It implies that a velocity-dependent self-interaction is preferred.

Z_h tends to be stable, while one can make the $\mathrm{U}(1)_h$-breaking scalar decay into two Z_h's. Thermally produced Z_h may overclose the Universe if it is stable. One may introduce a kinetic mixing between Z_h and the $\mathrm{U}(1)_Y$ hypercharge gauge boson so that Z_h can decay into an electron-positron pair or photons. However, late-time DM annihilation followed by the Z_h decay is largely disfavored by indirect detection constraints, e.g. from cosmic microwave background (CMB) anisotropies (see, e.g., ref. [9]). One way to avoid the overclosure of Z_h and these constraints is to make it decay only into standard model (SM) neutrinos.

A similar line of constructing a viable self-interacting DM model was pursued in ref. [10], where $\mathrm{U}(1)_h$ is identified as a flavoured lepton gauge symmetry $\mathrm{U}(1)_{L_\mu - L_\tau}$. The MeV-scale $L_\mu - L_\tau$ gauge boson decays predominantly into neutrinos since charged lepton channels are kinematically forbidden. On the other hand, the gauge coupling needs to be rather small to satisfy constraints from muon anomalous magnetic moment and thus the mediated self-interaction is also small. This is why the MeV-scale $\mathrm{U}(1)_{L_\mu - L_\tau}$-breaking scalar was considered as a scalar mediator of the DM self-interaction. In this paper, we propose a self-interacting DM model with a vector mediator [11–19].

We consider flavoured $\mathrm{U}(1)_{B-L}$ gauge symmetries; we introduce a $B-L$ gauge symmetry $\mathrm{U}(1)_{(B-L)_i}$ for each family ($i = 1, 2, 3$) in the SM sector. The anomaly cancellation implies that there is a right-handed neutrino N_{R_i} in each family. This model could be extended to grand unified theories such as $[SO(10)]^3$ [20] (see also ref. [21]). We assume that $\mathrm{U}(1)_{(B-L)_3}$ is spontaneously broken around the electroweak scale. MeV-scale Z_h decays predominantly into neutrinos through the kinetic mixing between Z_h and the $\mathrm{U}(1)_{(B-L))3}$ gauge boson $Z_{(B-L)_3}$ since channels into quarks and charged leptons are not kinematically allowed. In our model, we make the mass of the $\mathrm{U}(1)_h$-breaking scalar larger than $2 \times m_{Z_h}$ so that the scalar field can decay into two Z_h's. Quantum corrections give a kinetic mixing between $\mathrm{U}(1)_{(B-L)_3}$ and $\mathrm{U}(1)_Y$ gauge bosons because there are bicharged particles in the SM sector. Because of these kinetic mixings, our DM is within reach of direct detection experiments in the near future. In addition, the kinetic mixings make the DM annihilation lead to an electron-positron pair with a small branching ratio. Indirect detection experiments can potentially examine the signals.

Interestingly, we can realize the seesaw mechanism [22–25] and the thermal leptogenesis [26] (see, e.g., refs. [27–30] for recent reviews) by assuming $\mathrm{U}(1)_{(B-L)_1}$ and $\mathrm{U}(1)_{(B-L)_2}$ to be spontaneously broken at the scale above $10^9\,\mathrm{GeV}$. We assume that electroweak-scale N_{R_3} is stable because of a $\mathbb{Z}_2$ symmetry so as not to washout the $B-L$ asymmetry via its decay [31]. Our model can also explain the recent measurement of the lepton flavour universality violation in semi-leptonic B meson decays [32, 33] because the $\mathrm{U}(1)_{(B-L)_3}$ gauge boson mediates flavour universality violating interactions for mass eigenstates of quarks and leptons.

JHEP03(2019)021

This paper is organized as follows. First, we specify our model of DM and flavoured $\mathrm{U}(1)_{(B-L)_i}$. We introduce a spontaneously broken $\mathrm{U}(1)_h$ gauge symmetry in the dark sector. The $\mathrm{U}(1)_{(B-L)_3}$ is spontaneously broken around the electroweak scale so that the kinetic mixing with $Z_{(B-L)_3}$ leads to the decay of Z_h into SM neutrinos. In section 3, we discuss the cosmology of this model. In particular, we discuss that there are two candidates of DM in this model: the vector-like fermion in the hidden sector and N_{R_3}. The former one has the self-interaction through the massive gauge boson exchange and is assumed to be the dominant component of DM. Then, we discuss the compatibility with the present collider experiments and future detectability in section 4. Section 5 is devoted to the conclusion.

2 Model

We introduce three right-handed neutrinos N_{R_i} and flavoured $\mathrm{U}(1)_{(B-L)_i}$ gauge symmetries $(i = 1, 2, 3)$ that are spontaneously broken by vacuum expectation values (VEVs) of Φ_i at the energy scale of v_{ϕ_i}. We make the third family of right-handed neutrino stable by introducing a $\mathbb{Z}_2$ symmetry. We also introduce another complex scalar field Ψ and a vector-like fermion pair χ and $\bar{\chi}$ that are charged under a hidden gauge symmetry $\mathrm{U}(1)_h$. The field Ψ is assumed to obtain a nonzero VEV to break $\mathrm{U}(1)_h$ spontaneously at the energy scale of v_ψ. The charge of Ψ is taken to be three in units of that of χ to forbid Yukawa interactions with χ or $\bar{\chi}$. The charge assignment of the newly introduced particles is summarized in table 1, where we omit the first and second families for simplicity.

The Lagrangian is given by

$$\mathcal{L} = \mathcal{L}_{\mathrm{SM}} + \mathcal{L}_{\mathrm{kin}} + \mathcal{L}_{1,2} + \mathcal{L}_3 + \mathcal{L}_h \,, \tag{2.1}$$

$$\mathcal{L}_{1,2} = -\frac{1}{2}\sum_{i=1}^{2} y_{R_i}\Phi_i N_{R_i} N_{R_i} - \sum_{i=1}^{2} y_R^i H N_{R_i} L_i + \mathrm{h.c.} - \sum_{i=1}^{2} V_{\Phi_i}(\Phi_i) \,, \tag{2.2}$$

$$\mathcal{L}_3 = -\frac{1}{2} y_{R_3}\Phi_3 N_{R_3} N_{R_3} + \mathrm{h.c.} - V_{\Phi_3}(\Phi_3) \,, \tag{2.3}$$

$$\mathcal{L}_h = -m_\chi \chi\bar{\chi} + \mathrm{h.c.} - V_\Psi(\Psi) \,, \tag{2.4}$$

where $\mathcal{L}_{\mathrm{SM}}$ and $\mathcal{L}_{\mathrm{kin}}$ represent the SM Lagrangian and canonical kinetic terms of the newly introduced particles including the gauge interactions, respectively. H and L_i are the SM Higgs and lepton doublets, respectively. y_{R_i} and y_R^i $(y_R^3 = 0)$ are dimensionless Yukawa couplings.

The scalar fields are assumed to be unstable at the origins of the potentials, $V_{\Phi_i}(\Phi_i)$ and $V_\Psi(\Psi)$, and obtain nonzero VEVs v_{ϕ_i} and v_ψ at the stable minima. We denote the perturbations around the minima as ϕ_i and ψ as

$$\Phi_i = \frac{1}{\sqrt{2}}(v_{\phi_i} + \phi_i) \,, \tag{2.5}$$

$$\Psi = \frac{1}{\sqrt{2}}(v_\psi + \psi) \,. \tag{2.6}$$

After the spontaneous symmetry breaking (SSB), the gauge bosons $Z_{(B-L)_i}$ and Z_h obtain masses such as $m_{Z_{(B-L)_i}} = 2g_{(B-L)_i} v_{\phi_i}$ and $m_{Z_h} = 3g_h v_\psi$ with $g_{(B-L)_i}$ and g_h being

JHEP03(2019)021

	N_{R_3}	Φ_3	χ	$\bar{\chi}$	Ψ
$\mathrm{U}(1)_{(B-L)_3}$	-1	2	0	0	0
$\mathrm{U}(1)_h$	0	0	1	-1	3
$\mathbb{Z}_2$	-1	$+1$	$+1$	$+1$	$+1$

Table 1. Charge assignment.

the gauge couplings, respectively. The right-handed neutrinos obtain masses of $m_{N_{R_i}} = y_{R_i} v_{\phi_i}/\sqrt{2}$ via the Yukawa interaction. The SM neutrinos obtain small masses via the seesaw mechanism.

Because of the flavoured symmetry, the proper structure of Yukawa interactions cannot be generated in the simplest setup. To generate the proper Yukawa matrices, one may introduce (I) $\mathrm{U}(1)_{(B-L)_3}$-charged scalars in addition to $\mathrm{U}(1)_{(B-L)_3}$-neutral vector-like fermions that mix with the SM quarks and leptons [20]; or (II) an additional Higgs doublet that is charged under $\mathrm{U}(1)_{(B-L)_3}$ [34–36]. The additional fields lead to additional collider constraints on the model; e.g., vector-like fermions should be heavier than TeV [20]. We do not go into further detail about ultraviolet setups. We assume that after integrating out the heavy ($\sim$ TeV) fields, low-energy phenomenology is described by the above Lagrangian with the following Yukawa structure.

The SM Yukawa matrices can be diagonalized by a unitary rotation for each fermion: $f = U_f f'$ ($f = u_L, d_L, u_R, d_R, \nu_L, l_L, l_R$). Although each unitary matrix is not observable in the SM, except for $U_{u_L}^\dagger U_{d_L} = V_{\mathrm{CKM}}$ and $U_{l_L}^\dagger U_{\nu_L} = U_{\mathrm{PMNS}}$, it affects the interactions with the $Z_{(B-L)_3}$ boson. The interactions with the $Z_{(B-L)_3}$ boson are given by

$$\mathcal{L} \supset -\sum_f g_{(B-L)_3} Q_f Z^\mu_{(B-L)_3} J_{f,\mu}\,, \tag{2.7}$$

$$J_{f,\mu} = \sum_{i,j=1}^{3} \bar{f}_i (U_f)^*_{3i} (U_f)_{3j} \gamma_\mu f_j\,. \tag{2.8}$$

$Z_{(B-L)_3}$ can mediate interactions between different families in the mass eigenstate even if only the third family fermions are charged under $\mathrm{U}(1)_{(B-L)_3}$ in the interaction basis.

In this paper, we simply assume that the rotations of the right-handed fermions are suppressed and the 2-3 family rotations of the left-handed fermions exist in addition to V_{CKM} and U_{PMNS} such as

$$U_{l_L} = R_{23}(\theta_l)\,, \qquad U_{\nu_L} = R_{23}(\theta_l) U_{\mathrm{PMNS}}\,, \tag{2.9}$$

$$U_{d_L} = R_{23}(\theta_q)\,, \qquad U_{u_L} = R_{23}(\theta_q) V_{\mathrm{CKM}}^\dagger\,, \tag{2.10}$$

where $R_{23}(\theta)$ is a 2-3 family rotation by an angle θ. In particular we assume that $R_{13}(\theta)$ does not arise so that Z_h does not decay into electrons via the kinetic mixing with $Z_{(B-L)_3}$.

JHEP03(2019)021

3 Cosmology of the model

3.1 Thermal leptogenesis

We can generate the lepton asymmetry by the thermal leptogenesis via the decay of the first and second family right-handed neutrinos. We assume that the reheating temperature after the inflation is higher than the mass of the lighter one among these right-handed neutrinos so that they can be produced from the thermal plasma. The lepton asymmetry can be generated by their decay. Since the $B+L$ symmetry is broken by the non-perturbative effect, we can generate the baryon asymmetry from the lepton asymmetry. The observed baryon asymmetry can be explained when the lighter one is heavier than about $10^9\,\mathrm{GeV}$ [26].

If the third family right-handed neutrino has a Yukawa interaction with the SM particles, the $B-L$ symmetry violating interaction may be in equilibrium after the thermal leptogenesis and the lepton asymmetry may be washed out. To avoid this washout effect, we impose a $\mathbb{Z}_2$ symmetry on N_{R_3}. As a result, it is stable and can be a DM candidate.

If we do not introduce the $\mathbb{Z}_2$ symmetry on N_{R_3}, the Yukawa coupling with the SM fields y_R^3 should be small enough to suppress the washout effect. The decay rate of N_{R_3} is given by

$$\Gamma_{N_{R_3}} \simeq \frac{\left|y_R^3\right|^2}{8\pi} m_{N_{R_3}}\,. \tag{3.1}$$

The washout effect should not be efficient, $\Gamma_{N_{R_3}} \lesssim H$, until the temperature of the Universe decreases to the mass of N_{R_3}. Thus we require

$$|y_R^3| \lesssim 2\times 10^{-7}\left(\frac{m_{N_{R_3}}}{1\,\mathrm{TeV}}\right)^{1/2}, \tag{3.2}$$

to avoid the washout effect.

3.2 Dark matter

There are two DM candidates in our model. We identify χ and $\bar{\chi}$ as the dominant component of DM, while N_{R_3} is the subdominant component. Their thermal relic densities are determined as

$$\Omega_i h^2 \approx 0.12\left(\frac{3\times 10^{-26}\ \mathrm{cm^3 s^{-1}}}{(\sigma_i v)}\right), \tag{3.3}$$

with the s-wave annihilation cross section times relative velocity $(\sigma_i v)$ $(i = N_{R_3}, \chi)$.

3.2.1 Weakly-interacting DM: N_{R_3}

The annihilation of N_{R_3} proceeds through the $\mathrm{U}(1)_{(B-L)_3}$ gauge interaction and the Yukawa interaction with Φ_3. We found in ref. [31] that the dominant process is a s-wave annihilation channel $N_{R_3}N_{R_3} \to Z_{(B-L)_3}\phi_3$ if it is kinematically allowed and $m_{N_{R_3}} \gg m_{Z_{(B-L)_3}}, m_{\phi_3}$. The cross section is given by

$$\begin{aligned}(\sigma_{N_{R_3}} v)(N_{R_3}N_{R_3} \to Z_{(B-L)_3}\phi_3) \\ \simeq \frac{\pi\alpha_{(B-L)_3}^2}{4m_{N_{R_3}}^4 m_{Z_{(B-L)_3}}^4}\left[m_{\phi_3}^4 - 2m_{\phi_3}^2(4m_{N_{R_3}}^2 + m_{Z_{(B-L)_3}}^2) + (4m_{N_{R_3}}^2 - m_{Z_{(B-L)_3}}^2)^2\right]^{3/2},\end{aligned} \tag{3.4}$$

JHEP03(2019)021

where $\alpha_{(B-L)_3} \equiv g^2_{(B-L)_3}/(4\pi)$. The resulting amount of N_{R_3} can be then estimated as

$$\Omega_{N_{R_3}} h^2 \approx 1.4 \times 10^{-2} \left(\frac{m_{N_{R_3}}}{1\ \text{TeV}}\right)^{-2} \left(\frac{m_{Z_{(B-L)_3}}}{70\ \text{GeV}}\right)^{4} \left(\frac{\alpha_{(B-L)_3}}{10^{-4}}\right)^{-2} , \tag{3.5}$$

for $m_{N_{R_3}} \gtrsim m_{Z_{(B-L)_3}}, m_{\phi_3}$. We assume that N_{R_3} is the subdominant component of DM: $\Omega_{N_{R_3}} h^2 \ll (\Omega_{\rm DM} h^2)^{\rm obs} \approx 0.12$. Then we obtain

$$y_{R_3}^{-1} v_{\phi_3} \ll 2\,\text{TeV}\,. \tag{3.6}$$

The Yukawa coupling y_{R_3} cannot be arbitrary large because of the Unitarity bound. One may also require that the Landau pole does not appear below the Planck scale, which leads to $y_{R_3} \lesssim 1.2$ [31]. Then we obtain $v_{\phi_3} \ll 2.4\,\text{TeV}$ from eq. (3.6).

Although the dominant annihilation channel is s-wave and its cross section is not suppressed in the late Universe, N_{R_3} is not the dominant component of the DM and hence its indirect detection signals can be neglected.

3.2.2 Self-interacting DM: χ and $\bar{\chi}$

For χ and $\bar{\chi}$, the annihilation cross section is given by [37]

$$(\sigma_\chi v)(\chi\bar{\chi} \to Z_h Z_h) \simeq \frac{\pi \alpha_h^2}{m_\chi^2}\,, \tag{3.7}$$

$$(\sigma_\chi v)(\chi\bar{\chi} \to Z_h \psi) \simeq \frac{9\pi \alpha_h^2}{4 m_\chi^2}\,. \tag{3.8}$$

where $\alpha_h \equiv g_h^2/(4\pi)$. The total abundance of χ and $\bar{\chi}$ is twice larger than eq. (3.3) because there are χ and $\bar{\chi}$, each abundance of which is determined by the thermal freeze out. The resulting amount of χ and $\bar{\chi}$ can be then estimated as[1]

$$\Omega_\chi h^2 \approx 0.13 \left(\frac{m_\chi}{40\ \text{GeV}}\right)^2 \left(\frac{\alpha_h}{10^{-3}}\right)^{-2} . \tag{3.9}$$

The massive gauge boson Z_h mediates the self-interaction of χ and $\bar{\chi}$. It is convenient to use the transfer cross section defined by [39][2]

$$\sigma_T \equiv \frac{1}{2}\left(\sigma_T^{(\chi\chi)} + \sigma_T^{(\chi\bar{\chi})}\right) , \tag{3.10}$$

$$\sigma_T^{(\chi\chi),(\chi\bar{\chi})} = \int d\Omega (1-\cos\theta) \left(\frac{d\sigma^{(\chi\chi),(\chi\bar{\chi})}}{d\Omega}\right) . \tag{3.11}$$

When one computes σ_T, one encounters three regimes [39]: Born regime ($\alpha_h m_\chi/m_{Z_h} \ll 1$), classical regime ($\alpha_h m_\chi/m_{Z_h} \gtrsim 1$ & $m_\chi v_{\rm rel}/m_{Z_h} \gg 1$), and resonance regime ($\alpha_h m_\chi/m_{Z_h} \gtrsim$

[1] Depending on m_{Z_h}, the Sommerfeld enhancement can be significant [38]. When we focus on the regime where a large self-scattering cross section alleviates small-scale issues, $m_\chi \lesssim 100\,\text{GeV}$ is free from this subtlety.

[2] Replacing $1-\cos\theta$ by $1-|\cos\theta|$ is suggested since backward scattering has nothing to do with phase space redistribution as forward scattering [40, 41].

JHEP03(2019)021

1 & $m_\chi v_{\rm rel}/m_{Z_h} \lesssim 1$). In the Born regime, one can rely on the perturbative calculation and find an analytic expression in refs. [39, 41, 42]. In the classical and resonance regimes, one needs to solve the Schrödinger equation to take into account non-perturbative effects related to multiple exchanges of Z_h. Meanwhile, fitting formulas can be found in the classical regime [39, 42, 43, 43, 44]. In the resonance regime, an approximate formula can be obtained in the Hulthén potential [39].

Kinematics of dwarf and low-surface brightness galaxies indicate that $\sigma/m_\chi \approx$ 1-10 cm^2/g for the DM velocity of order 30 km/s [3]. On the other hand, observations of galaxy clusters prefer $\sigma_T/m_\chi \lesssim 0.1\,\mathrm{cm}^2/\mathrm{g}$ for the velocity of order 1000 km/s [3]. If the cross section saturates this upper bound, we can also explain the inferred density cores in the galaxy clusters [8]. The desirable parameter region is mostly in the resonance regime (see, e.g., ref. [10]), where the parameter dependence of the self-scattering cross section is non-trivial. In this paper, we do not pin down the precise values of m_χ and m_{Z_h} because they are not sensitive to other observables. Instead, we simply use an approximate formulas found in ref. [39] with the replacement of $\cos\theta \to |\cos\theta|$ in eq. (3.11) (see footnote 2) to check if the self-interaction cross section is within a desirable range. We find that the above constraints can be satisfied when $m_{Z_h} \approx$ 10-100 MeV and $m_\chi \approx$ 10-100 GeV.

3.3 Dark radiation

We assume that the mass of the dark Higgs boson ψ is larger than twice that of Z_h, so that it can decay into two Z_h's. We make Z_h unstable by introducing a kinetic mixing between $\mathrm{U}(1)_{(B-L)_3}$ and $\mathrm{U}(1)_h$:

$$-\frac{1}{2}\epsilon_2 F^{\mu\nu}_{(B-L)_3} F_{h\,\mu\nu}\,, \tag{3.12}$$

where $F_{(B-L)_3}$ and F_h denote the field strengths of $\mathrm{U}(1)_{(B-L)_3}$ and $\mathrm{U}(1)_h$, respectively. Then Z_h can decay into third family neutrinos ν_3 via the mixing with $Z_{(B-L)_3}$. We remark that the decay of Z_h into muons μ or taus τ is kinematically forbidden for $m_{Z_h} \lesssim 200\,\mathrm{MeV}$. The other decay of Z_h into electrons e is suppressed since $Z_{(B-L)_3}$ does not directly couple to e under our assumption of the Yukawa structure [see eq. (2.9)]. Thus the late time DM annihilation into Z_h results in ν_3 and thus is harmless.

The decay rate can be estimated as

$$\Gamma_{Z_h} \sim \alpha_{(B-L)_3}\epsilon_2^2 \left(\frac{m_{Z_h}}{m_{Z_{(B-L)_3}}}\right)^4 m_{Z_h}\,. \tag{3.13}$$

We require that Z_h decays into ν_3 long before the neutrino decoupling; otherwise only the temperature of ν_3 is enhanced by the decay of Z_h and the energy density of ν_3 may exceed the upper bound on that of dark radiation. This can be satisfied when $\Gamma_{Z_h} \gtrsim H|_{T=1\,\mathrm{MeV}}$, where H is the Hubble expansion rate at temperature T. It gives the lower bound on the mixing parameter as

$$\epsilon_2 \gtrsim 4\times 10^{-2}\left(\frac{m_{Z_{(B-L)_3}}}{70\,\mathrm{GeV}}\right)^2\left(\frac{m_{Z_h}}{10\,\mathrm{MeV}}\right)^{-5/2}\left(\frac{\alpha_{(B-L)_3}}{10^{-4}}\right)^{-1/2}. \tag{3.14}$$

JHEP03(2019)021

Even if Z_h decays into ν_3 long before the neutrino decoupling, the thermalized Z_h can still enhance only the temperature of ν_3 after the neutrino decoupling. This constraint is evaded for $m_{Z_h} \gtrsim 10\,\mathrm{MeV}$ [10, 45].

Furthermore, one needs to take account of Z_h possibly dominating the energy density of the Universe. It takes place if the decay rate of the $\mathrm{U}(1)_h$ gauge boson is much smaller than the Hubble expansion rate when the temperature is comparable to the mass of the $\mathrm{U}(1)_h$ gauge boson, $\Gamma_{Z_h} \lesssim H|_{T=m_{Z_h}}$. If $m_{Z_h} > 1\,\mathrm{MeV}$ and $\Gamma_{Z_h} \lesssim H|_{T=1\,\mathrm{MeV}}$, the Hubble expansion rate during the big bang nucleosynthesis is dominated by non-relativistic Z_h and affects the big bang nucleosynthesis critically.[3] If $m_{Z_h} > 1\,\mathrm{MeV}$ and $\Gamma_{Z_h} \gtrsim H|_{T=1\,\mathrm{MeV}}$, the Z_h domination does not impact the big bang nucleosynthesis, but still dilutes the baryon asymmetry. To avoid such a wash out, the lower bound of the mixing should satisfy

$$\epsilon_2 \gtrsim 4 \times 10^{-1} \left(\frac{m_{Z_{(B-L)_3}}}{70\,\mathrm{GeV}}\right)^2 \left(\frac{m_{Z_h}}{10\,\mathrm{MeV}}\right)^{-3/2} \left(\frac{\alpha_{(B-L)_3}}{10^{-4}}\right)^{-1/2} . \tag{3.15}$$

If this condition is not satisfied, the amount of the entropy production due to the Z_h decay can be estimated as

$$\Delta \equiv \frac{s_f a_f^3}{s_i a_i^3} \simeq \frac{m_{Z_h}}{T_d} \tag{3.16}$$

$$\approx 10 \left(\frac{\epsilon_2}{4 \times 10^{-2}}\right)^{-1} \left(\frac{m_{Z_{(B-L)_3}}}{70\,\mathrm{GeV}}\right)^2 \left(\frac{m_{Z_h}}{10\,\mathrm{MeV}}\right)^{-3/2} \left(\frac{\alpha_{(B-L)_3}}{10^{-4}}\right)^{-1/2} , \tag{3.17}$$

where $a_i(a_f)$ and $s_i(s_f)$ are the scale factor and entropy density before (after) the Z_h domination, respectively, and T_d is the decay temperature of Z_h. The constraint (3.15) can be evaded if the generated baryon asymmetry is larger than the observed value by this factor. This can be realized when the first and second right-handed neutrinos are heavier than $10^9\,\mathrm{GeV}$ at least by the same factor.

Here we comment on another possible mechanism of the entropy production, which could be relevant in models with a spontaneous symmetry breaking. As for a dynamics of $\mathrm{U}(1)_h$ breaking in the hidden sector, a thermal inflation may occur at the time of the phase transition if the mass of the gauge boson m_{Z_h} is many orders of magnitude larger than that of the symmetry-breaking field m_ψ. This effect washes out the baryon asymmetry, so that we should avoid such a thermal inflation. We discuss the condition to avoid a thermal inflation in appendix B and check that it does not occur in our model. However, we note that it is non-trivial in other models with hierarchical mass scales.

3.4 DM direct and indirect detection constraints

There may be couplings between scalar fields like $\lambda_{H\Phi_i} |H|^2 |\Phi_i|^2$ and $\lambda_{H\Psi} |H|^2 |\Psi|^2$. Since they are irrelevant in the above discussion, we take the loop induced values as natu-

[3] This point seems missing in ref. [37], where the lightest particle in a hidden sector (Z_h in our case) is the dark Higgs boson. They take about 1.5 MeV as a reference value of the dark Higgs boson mass and require its lifetime to be shorter than $10^5\,\mathrm{s}$ not to affect the CMB spectral distortion (see, e.g., ref. [46]). However, the lifetime of the dark Higgs boson should be shorter than $\mathcal{O}(1)\,\mathrm{s}$ not to dominate the energy density of the Universe if the dark sector is decoupled from the SM sector after the QCD phase transition. In ref. [47], they have investigated this effect in detail and found that the lifetime can be as long as $\mathcal{O}(100)\,\mathrm{s}$ for the $\mathcal{O}(1)\,\mathrm{MeV}$ dark Higgs boson if it is decoupled before the QCD phase transition.

JHEP03(2019)021

ral choices. For example, the former interaction arises at the two loop level as $\lambda_{H\Phi_3} \sim y_t^2 \alpha_{(B-L)_3}^2/(4\pi)^2$. It results in the mixing between the SM Higgs and ϕ, which leads to spin-independent N_{R_3}-nucleon scatterings. However, N_{R_3} is the subdominant component of DM and hence easily evades the constraint from the direct detection experiments for DM. For the same reason, the indirect detection constraint on N_{R_3} is also weakened.

The kinetic mixing between the $\mathrm{U}(1)_Y$ and $\mathrm{U}(1)_{(B-L)_3}$ gauge bosons arises at the one-loop level:

$$\mathcal{L}_{\rm kin} \supset -\frac{1}{2}\epsilon_1 F_{Y\,\mu\nu} F^{\mu\nu}_{(B-L)_3}\,, \tag{3.18}$$

$$\epsilon_1 \simeq \frac{2 g_Y g_{(B-L)_3}}{9\pi^2} \ln\left(\frac{\Lambda}{\mu}\right) \approx 10^{-2} \left(\frac{\alpha_{(B-L)_3}}{10^{-4}}\right)^{1/2} \ln\left(\frac{\Lambda}{10^{16}\,\mathrm{GeV}} \frac{10^2\,\mathrm{GeV}}{\mu}\right)\,, \tag{3.19}$$

where $F_{Y\,\mu\nu}$ and g_Y are the field strength and gauge coupling for $\mathrm{U}(1)_Y$, respectively. Here μ is the energy scale considered and Λ is a cutoff scale at which the kinetic mixing vanishes. When $\mathrm{U}(1)_Y$ is unified into a non-abelian gauge symmetry, we should take Λ to be the grand unification scale of order $10^{16}\,\mathrm{GeV}$.[4] Through the kinetic mixings parametrized by ϵ_1 and ϵ_2, we obtain effective interactions between χ and SM particles as calculated in appendix A. In particular, there is the following effective interaction at a low energy scale:

$$\mathcal{L} \supset b_p \bar{\chi}\gamma^\mu \chi \bar{p}\gamma_\mu p\,, \tag{3.20}$$

where p represents the proton. From eq. (A.24) and the discussion below the equation, we estimate the coefficient b_p roughly as

$$b_p \sim \frac{e g_h \cos\theta_W \epsilon_1 \epsilon_2}{m^2_{Z_{(B-L)_3}}} f(q^2/m^2_{Z_h})\,, \tag{3.21}$$

where e is the electromagnetic charge, q^2 is the squared momentum transfer, and

$$f(x) = \frac{x}{1+x}\,. \tag{3.22}$$

The momentum transfer is of order $\mu v_{\rm DM}$, where μ ($\sim m_\chi$) is the reduced mass for χ and the nucleus and $v_{\rm DM}$ ($\sim 10^{-3}$) is the relative velocity. Noting that $m_{Z_h}/m_\chi \sim 10^{-3}$, we expect $f(q^2/m^2_{Z_h}) = \mathcal{O}(1)$.

For a given nucleus ${}^A_Z N$, the coefficient of the coupling is given by $b_N = Z b_p$, where we neglect the contribution comes from the neutron. Then the spin-independent χ-nucleon scattering cross section is given by

$$\sigma_N = \frac{1}{\pi}\frac{\mu_N^2}{A^2} b_N^2 \tag{3.23}$$

$$\sim 7\times 10^{-48}\,\mathrm{cm}^2 \times f(q^2/m^2_{Z_h}) \left(\frac{\alpha_h}{10^{-3}}\right) \left(\frac{\epsilon_1}{10^{-2}}\right)^2 \left(\frac{\epsilon_2}{10^{-2}}\right)^2 \left(\frac{m_{Z_{(B-L)_3}}}{70\,\mathrm{GeV}}\right)^{-4}\,, \tag{3.24}$$

[4] We implicitly consider $\mathrm{SU}(5)\times\mathrm{U}(1)_{(B-L)_3}\times\mathrm{U}(1)_h$ gauge theory as an effective theory, where SU(5) breaks down to the SM gauge groups at the GUT scale. In this case, the kinetic mixing between the $\mathrm{U}(1)_Y$ and $\mathrm{U}(1)_h$ gauge bosons are forbidden above the GUT scale while the one between the $\mathrm{U}(1)_{(B-L)_3}$ and $\mathrm{U}(1)_h$ gauge bosons is allowed by the symmetry, $\mathrm{SU}(5)\times\mathrm{U}(1)_{(B-L)_3}\times\mathrm{U}(1)_h$. Although the former one can be induced after the GUT symmetry breaking, it depends on the detail of the model. In this paper, we assume that the mixing parameter is suppressed enough so that our DM can evade the constraints coming from DM direct detection experiments.

JHEP03(2019)021

(see, e.g., ref. [48]), where μ_N is the χ-nucleon reduced mass. This is just below the present upper bound reported by XENON1T for $m_\chi = 20$–$100\,\mathrm{GeV}$ [49]. XENONnT [50], DarkSide-20k [51], and LUX-ZEPLIN [52] can search DM with a cross section smaller by a factor of order 10. DARWIN can detect DM if the cross section is above the neutrino coherent scattering cross section [53], which is around $10^{-49}\,\mathrm{cm}^2$ for $m_\chi = 20$–$100\,\mathrm{GeV}$.

As we stressed, the late-time annihilation of the dominant component of DM, χ and $\bar{\chi}$, predominantly results in ν_3. Since the detection of neutrino signals is quite challenging and the constraint is very weak [54], this does not lead to observable effects on astrophysical experiments. However, their annihilation can also result in an electron-positron pair via the process of $Z_h \to e\bar{e}$. The branching ratio is calculated from eq. (A.24) and the result is given by

$$\mathrm{Br}\,(Z_h \to e\bar{e}) \simeq 2c_W^2\epsilon_1^2\frac{\alpha}{\alpha_h} \tag{3.25}$$

$$\approx 10^{-3}\left(\frac{\epsilon_1}{10^{-2}}\right)^2\left(\frac{\alpha_h}{10^{-3}}\right)^{-1}, \tag{3.26}$$

where $\alpha = e^2/(4\pi)$. The effective annihilation cross section of DM into electron-positron pairs is given by

$$(\sigma_\chi v)(\chi\bar{\chi} \to e\bar{e}\cdots) \simeq S\,[2\mathrm{Br} \times (\sigma_\chi v)(\chi\bar{\chi} \to Z_h Z_h) + \mathrm{Br} \times (\sigma_\chi v)(\chi\bar{\chi} \to Z_h\psi)] \tag{3.27}$$

$$\approx 1.1 \times 10^{-28}\,\mathrm{cm}^3/\mathrm{s}\,S\left(\frac{\epsilon_1}{10^{-2}}\right)^2\left(\frac{m_\chi}{40\ \mathrm{GeV}}\right)^2\left(\frac{\alpha_h}{10^{-3}}\right)^{-3}, \tag{3.28}$$

where S represents a Sommerfeld enhancement factor. An upper bound on the annihilation cross section into an electron-positron pair is obtained from AMS-02 data as $\mathcal{O}(1) \times 10^{-26}\,\mathrm{cm}^3/\mathrm{s}$ for $m_\chi = \mathcal{O}(10)\,\mathrm{GeV}$ ($\approx 1 \times 10^{-26}\,\mathrm{cm}^3/\mathrm{s}$ for $m_\chi = 40\,\mathrm{GeV}$) [55].[5] We calculate the Sommerfeld enhancement factor by using the Hulthén potential as done in ref. [56]. The result is typically $\mathcal{O}(1)$ for $v \sim 100\,\mathrm{km/s}$ ($S \approx 3$ for $m_\chi = 40\,\mathrm{GeV}$, $\alpha_h = 10^{-3}$, and $m_{Z_h} = 10\,\mathrm{MeV}$). The Sommerfeld enhancement factor increases toward lower velocity and saturate at

$$S \approx 50\left(\frac{m_\chi}{40\,\mathrm{GeV}}\right)\left(\frac{\alpha_h}{10^{-3}}\right)\left(\frac{m_{Z_h}}{10\,\mathrm{MeV}}\right)^{-1} \tag{3.29}$$

unless a parameter is tuned to enhance it resonantly. The resultant cross section is close to an upper bound from CMB anisotropies [55], $\mathcal{O}(1) \times 10^{-25}\,\mathrm{cm}^3/\mathrm{s}$ ($\approx 8 \times 10^{-26}\,\mathrm{cm}^3/\mathrm{s}$ for $m_\chi = 40\,\mathrm{GeV}$). In summary, the present constraints on indirect detection are already constraining some parameter space. We expect that indirect detection experiments with a large exposure and a better understanding of cosmic ray background and propagation will examine a broader parameter space.

4 Collider constraints

As discussed in section 2, we assume that the appropriate flavour structure of the SM Yukawa matrices comes from some UV physics (see, e.g., ref. [20]). The CKM and PMNS

[5] In ref. [55], they consider the case of Majorana DM while we consider Dirac DM. To compare the result, we multiply the upper bound by a factor of 2.

JHEP03(2019)021

matrices are attributed to the left-handed up-type quarks and neutrinos, respectively. We allow for additional 2-3 family rotations of left-handed quarks and leptons.

4.1 No additional physical phase

First we discuss the constraints from collider experiments, when there are no additional physical phases, $\theta_l = \theta_q = 0$, following ref. [31].

A relevant constraint on the $Z_{(B-L)_3}$ mass comes from the lepton flavour universality violation in Υ decays. The lepton flavour universality ratio is modified in the presence of $Z_{(B-L)_3}$ as

$$R_{\tau\mu}(\Upsilon(1S)) \equiv \frac{\Gamma_{\Upsilon(1S)\to\tau\bar{\tau}}}{\Gamma_{\Upsilon(1S)\to\mu\bar{\mu}}} \tag{4.1}$$

$$\simeq \left(1 + \frac{\alpha_{(B-L)_3}}{\alpha} \frac{m_\Upsilon^2}{m_{Z_{(B-L)_3}}^2 - m_\Upsilon^2}\right)^2 , \tag{4.2}$$

where m_Υ ($\approx 9.46\,\mathrm{GeV}$) is the Upsilon mass. The BaBar experiment places the constraint on this ratio as $R_{\tau\mu} = 1.005 \pm 0.013(\mathrm{stat.}) \pm 0.022(\mathrm{syst.})$ [57]. In the limit of $m_{Z_{(B-L)_3}}^2 \gg m_\Upsilon^2$, we obtain

$$\left(\frac{m_{Z_{(B-L)_3}}}{70\,\mathrm{GeV}}\right)^2 \left(\frac{\alpha_{(B-L)_3}}{10^{-4}}\right)^{-1} \gtrsim 1.7 \times 10^{-2} , \tag{4.3}$$

corresponding to

$$v_{\phi_3} \gtrsim 130\,\mathrm{GeV} . \tag{4.4}$$

This is consistent with the upper bound on v_{ϕ_3} from the N_{R_3} abundance [see eq. (3.6)].

Since the $\mathrm{U}(1)_{(B-L)_3}$ gauge boson is coupled with the third-family quarks, it can be produced in hadron colliders. The dominant production process is a Drell-Yan process from the bottom quark pair: $b\bar{b} \to Z_{(B-L)_3}$. Resonance searchs in the $\tau\bar{\tau}$ final state place the constraint for $200\,\mathrm{GeV} \lesssim m_{Z_{(B-L)_3}} \lesssim 4\,\mathrm{TeV}$ [58]. This constraint, $\alpha_{(B-L)_3} \lesssim 10^{-3}$ for $m_{Z_{(B-L)_3}} \sim 200\,\mathrm{GeV}$, would not be quite stringent when compared to others.[6]

The kinetic mixing between the $Z_{(B-L)_3}$ and $\mathrm{U}(1)_Y$ gauge bosons changes the mass eigenstates and interactions of the vector mesons. In particular it leads to a shift in the SM Z boson mass. In the mass basis, the physical mass of the SM Z boson, denoted by m_{Z_1}, is given by eq. (A.17). The mass of the SM Z boson is tightly constrained by electroweak precision measurements and is consistent with the SM prediction. In this paper we require that the mass difference is smaller than the current experimental uncertainty of $0.0021\,\mathrm{GeV}$ [61]. The kinetic mixing parameter ϵ_1 can be written in terms of $\alpha_{(B-L)_3}$ as in eq. (3.19). Then we can plot a constraint in the $\alpha_{(B-L)_3}$-$m_{Z_{(B-L)_3}}$ plane as shown by the blue region in figure 1. The orange region in the upper left corner is excluded by the Υ decay measurement. We also plot a green region that is excluded by the flavour physics as we will discuss in section 4.2. The dashed lines are a couple of reference parameter values that we will use in figure 2.

[6] Our reference value of $m_{Z_{(B-L)_3}}$ is $70\,\mathrm{GeV}$, which is slightly out of this range. We expect that the constraint does not change drastically (see also refs. [59, 60]).

JHEP03(2019)021

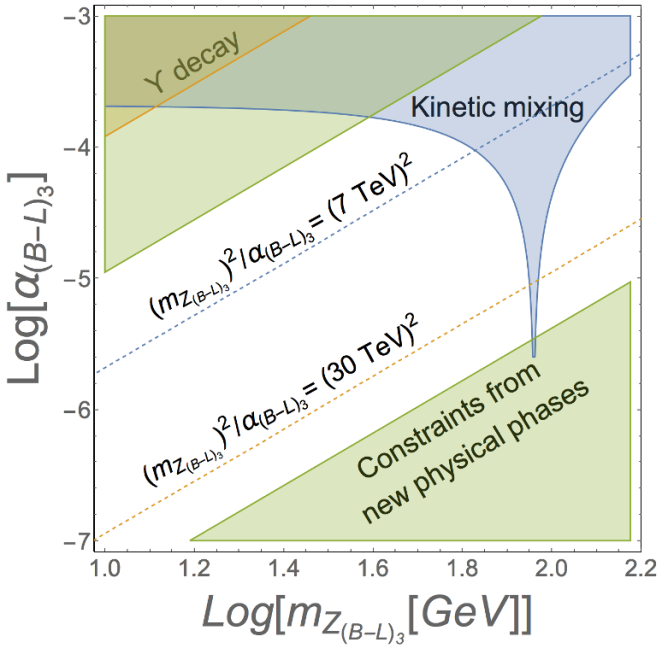

Figure 1. Parameter region in the $\alpha_{(B-L)_3}$-$m_{Z_{(B-L)_3}}$ plane. The orange and blue shaded regions are constrained by the Υ decay and kinetic mixing, respectively, when $\theta_l = \theta_q = 0$. In the green shaded regions, one cannot find a region in the $\sin\theta_l$-$\sin\theta_q$ plane, where the flavour constraints are satisfied. The dashed lines are the reference parameter values that we use in figure 2.

The Higgs-portal interaction $\lambda_{H\Phi_3}|H|^2|\Phi_3|^2$ may provide indirect signals of Higgs invisible decays if the SM Higgs can decay into $N_{R_3}N_{R_3}$, $Z_{(B-L)_3}Z_{(B-L)_3}$, or $\phi_3\phi_3$. The constraint, however, can be easily evaded unless the Higgs-portal coupling is as large as $\mathcal{O}(1)$.

4.2 Non-zero new physical phases

Next we allow the additional physical phases to be non-zero. The following discussion is based on ref. [20].

4.2.1 Semi-leptonic B decays

To study semi-leptonic B decays, it is convenient to use the following effective Hamiltonian at the low energy:

$$\mathcal{H}_{\text{eff}} = -\frac{4G_F}{\sqrt{2}}V_{tb}V_{ts}^*\left(\sum_{l=e,\mu,\tau}\left(C_9^l\mathcal{O}_9^l + C_{10}^l\mathcal{O}_{10}^l\right) + \sum_{i,j=1}^{3}C_\nu^{ij}\mathcal{O}_\nu^{ij}\right), \tag{4.5}$$

$$\mathcal{O}_9^l = \frac{\alpha}{4\pi}\left(\bar{s}\gamma_\mu b_L\right)\left(\bar{l}\gamma_\mu l\right), \tag{4.6}$$

$$\mathcal{O}_{10}^l = \frac{\alpha}{4\pi}\left(\bar{s}\gamma_\mu b_L\right)\left(\bar{l}\gamma_\mu\gamma^5 l\right), \tag{4.7}$$

$$\mathcal{O}_\nu^{ij} = \frac{\alpha}{2\pi}\left(\bar{s}\gamma_\mu b_L\right)\left(\bar{\nu}_i\gamma_\mu\nu_{L\,j}\right). \tag{4.8}$$

JHEP03(2019)021

After integrating out $Z_{(B-L)_3}$, we obtain the deviation from the SM contributions for μ such as

$$\delta C_9^\mu = -\delta C_{10}^\mu = -\frac{\pi}{\alpha\sqrt{2}G_F V_{tb}V_{ts}^*}\frac{g_{(B-L)_3}^2 s_{\theta_q}c_{\theta_q}s_{\theta_l}^2}{3m_{Z_{(B-L)_3}}^2}\,, \tag{4.9}$$

where V_{tb} denotes the tb component of $V_{\rm CKM}$ and so on. Hereafter, we also use $s_{\theta_q} \equiv \sin\theta_q$ and so on. The LHCb experiment reported the lepton flavour universality violation in semi-leptonic B decays [32, 33], which is represented by the ratio of

$$\mathcal{R}_K^{(*)} = \frac{\Gamma(B\to K^{(*)}\mu\bar{\mu})}{\Gamma(B\to K^{(*)}e\bar{e})}\,. \tag{4.10}$$

The tension with the SM prediction is around the 4σ level [62–68]. This can be explained by the $Z_{(B-L)_3}$ contribution when $\delta C_9^\mu \in [-0.81, -0.48]$ (1σ interval) [69]. Using $|V_{tb}| \approx 1.0$ and $|V_{ts}| \approx 3.9\times10^{-2}$ [61], we then require

$$8.7\times10^{-3} \lesssim s_{\theta_q}c_{\theta_q}s_{\theta_l}^2\left(\frac{\alpha_{(B-L)_3}}{10^{-4}}\right)\left(\frac{m_{Z_{(B-L)_3}}}{70\,\mathrm{GeV}}\right)^{-2} \lesssim 1.5\times10^{-2}\,. \tag{4.11}$$

The B meson can decay also into neutrinos: $B\to K^{(*)}\nu\bar{\nu}$. The deviation from the SM contribution is given by

$$\delta C_\nu^{ij} = \delta C_\nu\,(U_{\nu_L})_{3i}^*\,(U_{\nu_L})_{3j}\,, \tag{4.12}$$

$$\delta C_\nu = -\frac{\pi}{\alpha\sqrt{2}G_F V_{tb}V_{ts}^*}\frac{g_{(B-L)_3}^2 s_{\theta_q}c_{\theta_q}}{3m_{Z_{(B-L)_3}}^2}\,. \tag{4.13}$$

The ratio to the SM prediction is given by

$$R_{\nu\bar{\nu}} \equiv \frac{\Gamma}{\Gamma_{\rm SM}} = 1 + \frac{2}{3}\left(\frac{\delta C_\nu}{C_\nu^{(\rm SM)}}\right) + \frac{1}{3}\left(\frac{\delta C_\nu}{C_\nu^{(\rm SM)}}\right)^2\,, \tag{4.14}$$

where $C_\nu^{(\rm SM)} \approx -6.35$ [70]. The experimental upper bound is $R_{\nu\bar{\nu}} < 4.3$ at the 90% confidence level (CL) [71, 72], which gives

$$s_{\theta_q}c_{\theta_q}\left(\frac{\alpha_{(B-L)_3}}{10^{-4}}\right)\left(\frac{m_{Z_{(B-L)_3}}}{70\,\mathrm{GeV}}\right)^{-2} \lesssim 2.6\times10^{-1}\,. \tag{4.15}$$

Combining this with eq. (4.11), we obtain

$$|s_{\theta_l}| \gtrsim 0.18\,. \tag{4.16}$$

4.2.2 B_s-$\bar{B}_s$ and D^0-$\bar{D}^0$ mixings

$Z_{(B-L)_3}$ also contributes to the B_s-$\bar{B}_s$ mixing via the following effective Lagrangian:

$$\mathcal{L} \supset -\frac{g_{(B-L)_3}^2 s_{\theta_q}^2 c_{\theta_q}^2}{18m_{Z_{(B-L)_3}}^2}\,(\bar{s}\gamma^\mu b_L)^2\,. \tag{4.17}$$

JHEP03(2019)021

This gives a deviation of the B meson mass difference from the SM prediction as

$$C_{B_s} \equiv \frac{\Delta m_{B_s}}{\Delta m_{B_s}^{(\mathrm{SM})}} = 1 + \frac{4\pi^2 c(m_{Z_{(B-L)_3}})}{G_F^2 m_W^2 V_{tb} V_{ts}^* \hat{\eta}_B S(m_t^2/m_W^2)} \frac{g_{(B-L)_3}^2 s_{\theta_q}^2 c_{\theta_q}^2}{18 m_{Z_{(B-L)_3}}^2}\,, \tag{4.18}$$

where $c(m_{Z_{(B-L)_3}}) \approx 0.8$ [73, 74], $S(m_t^2/m_W^2) \approx 2.30$ [75], and $\hat{\eta}_B \approx 0.84$ [76, 77]. The experimental constraint is $0.899 < C_{B_s} < 1.252$ (95% CL interval) [78]. Then we obtain

$$\left|s_{\theta_q} c_{\theta_q}\right| \left(\frac{\alpha_{(B-L)_3}}{10^{-4}}\right)^{1/2} \left(\frac{m_{Z_{(B-L)_3}}}{70\,\mathrm{GeV}}\right)^{-1} \lesssim 2.0 \times 10^{-1}\,. \tag{4.19}$$

This upper bound is comparable to that in eq. (4.15), in the parameter region that we are interested in.

The D^0-$\bar{D}^0$ mixing is induced by the $Z_{(B-L)_3}$ exchange effective interaction of

$$\mathcal{L} \supset -\frac{g_{(B-L)_3}^2 c_D^2}{18 m_{Z_{(B-L)_3}}^2} \left(\bar{u}\gamma^\mu c_L\right)^2\,, \tag{4.20}$$

where

$$c_D \equiv \left(V_{ub} c_{\theta_q} - V_{us} s_{\theta_q}\right)\left(V_{cb}^* c_{\theta_q} - V_{cs}^* s_{\theta_q}\right)\,. \tag{4.21}$$

This results in a new physics contribution of

$$\Delta m_D^{\mathrm{NP}} = \frac{2}{3} f_D^2 B_D m_D\, c(m_{Z_{(B-L)_3}}) \frac{g_{(B-L)_3}^2 c_D^2}{18 m_{Z_{(B-L)_3}}^2}\,, \tag{4.22}$$

where $f_D \approx 207.4\,\mathrm{MeV}$ [79] and $B_D \approx 0.757$ [80] are calculated by the lattice quantum chromodynamics. The D^0 meson mass is $m_D \approx 1.86\,\mathrm{GeV}$. The mass difference calculated in the SM has large uncertainties [81], so that we cannot evaluate the total (SM + NP) mass difference robustly. In this paper we simply require that the new physics contribution does not exceed the experimental data, which is $4 \times 10^{-4} < \Delta m_D^{\mathrm{NP}}/\Gamma < 6.2 \times 10^{-3}$, where $\Gamma \approx 2.44 \times 10^{12}\,/\mathrm{s}$ is the average decay width of D^0 and $\bar{D}^0$ [61, 82]. Since $|V_{ub}| \approx 4.1 \times 10^{-3}$, $|V_{us}| \approx 0.22$, $|V_{cb}| \approx 4.1 \times 10^{-2}$, and $|V_{cs}| \approx 1.0$, this constraint is stringent particularly for $c_{\theta_q} \ll 1$. Then we obtain

$$\left|s_{\theta_q}\right| \left(\frac{\alpha_{(B-L)_3}}{10^{-4}}\right)^{1/4} \left(\frac{m_{Z_{(B-L)_3}}}{70\,\mathrm{GeV}}\right)^{-1/2} \lesssim 1.5 \times 10^{-1} \tag{4.23}$$

for $s_{\theta_q} \gg 0.04 c_{\theta_q}$.

4.2.3 Lepton flavour violation

Lepton flavour violating processes are also induced by $Z_{(B-L)_3}$ interactions. The most important effective interaction is

$$\mathcal{L} \supset \frac{g_{(B-L)_3}^2}{m_{Z_{(B-L)_3}}^2} s_{\theta_l}^3 c_{\theta_l} \bar{\tau}\gamma^\rho \mu_L \bar{\mu}\gamma_\rho \mu_L\,, \tag{4.24}$$

JHEP03(2019)021

which gives the τ decay into 3μ. The resulting branching ratio is given by

$$\mathcal{B}r(\tau \to 3\mu) = \frac{m_\tau^5}{48\pi\Gamma_\tau} \frac{\alpha_{(B-L)_3}^2}{m_{Z_{(B-L)_3}}^4} s_{\theta_l}^6 c_{\theta_l}^2 \,, \tag{4.25}$$

where m_τ ($\approx 1.78\,\mathrm{GeV}$) and $\Gamma_\tau \approx (2.9 \times 10^{-13}\,\mathrm{s})^{-1} \approx 2.3 \times 10^{-12}\,\mathrm{GeV}$ are the mass and decay width of the tau lepton, respectively. The experimental upper bound is $\mathcal{B}r(\tau \to 3\mu) < 2.1 \times 10^{-8}$ at the 90% CL [83]. Thus we obtain

$$\left|s_{\theta_l}^3 c_{\theta_l}\right| \left(\frac{\alpha_{(B-L)_3}}{10^{-4}}\right) \left(\frac{m_{Z_{(B-L)_3}}}{70\,\mathrm{GeV}}\right)^{-2} \lesssim 3.1 \times 10^{-2} \,. \tag{4.26}$$

For the reference parameter values, $\alpha_{(B-L)_3} = 10^{-4}$ and $m_{Z_{(B-L)_3}} = 70\,\mathrm{GeV}$, this constraint implies that $|s_{\theta_l}| \lesssim 0.32$, which is compatible with eq. (4.16).

4.2.4 $Z_{(B-L)_3}$ production and decay in colliders

The mixing in the lepton sector leads to new decay channels of $Z_{(B-L)_3}$: $Z_{(B-L)_3} \to \mu\bar{\mu}$ and $Z_{(B-L)_3} \to \mu\tau$. We can place a constraint by using the dimuon search by the ATLAS and CMS collaborations at the LHC experiment for $200\,\mathrm{GeV} < m_{Z_{(B-L)_3}} < 4\,\mathrm{TeV}$ [84, 85]. The constraint is similar to $Z_{(B-L)_3} \to \tau\bar{\tau}$ discussed in section 4.1 and would not be quite stringent.

The SM Z boson can decay into $\mu\bar{\mu}Z_{(B-L)_3}$ followed by $Z_{(B-L)_3} \to \mu\bar{\mu}$. The ATLAS collaboration reported an upper bound on the branching ratio of $Z \to 4\mu$ as $\mathcal{B}r(Z \to 4\mu) < [3.2 \pm 0.25(\mathrm{stat.}) \pm 0.13(\mathrm{syst.})] \times 10^{-6}$ [86]. This can be interpreted as an upper bound on $g_{(B-L)_3} s_{\theta_l}^4$ for a given $m_{Z_{(B-L)_3}}$, where $g_{(B-L)_3} s_{\theta_l}^2$ comes from a coupling for the $Z_{(B-L)_3}$ production process and another $s_{\theta_l}^2$ comes from a branching ratio of $Z_{(B-L)_3}$ decay into $\mu\bar{\mu}$.[7] We simply estimate the constraint by replacing g' of figure 1 of ref. [87] with our $g_{(B-L)_3} s_{\theta_l}^4/3^2$, where a factor of 3^2 comes from a difference of the charge between the models. The resulting constraint is $g_{(B-L)_3} s_{\theta_l}^4 \lesssim 6 \times 10^{-2}$ for $m_{Z_{(B-L)_3}} = 20$-$30\,\mathrm{GeV}$, while it is two orders of magnitude weaker for $m_{Z_{(B-L)_3}} \gtrsim 70\,\mathrm{GeV}$. We find that this constraint is negligible in most of the parameter region that we are interested in.

Because of the kinetic mixing, $Z_{(B-L)_3}$ can be produced by hadron colliders via the Drell-Yan process, which leads to a clear dilepton signal with an invariant mass about the $Z_{(B-L)_3}$ boson mass. In ref. [88], they considered the case where a hidden gauge boson is coupled with the SM sector only via the kinetic mixing and estimated that the 8 TeV LHC with $20\,\mathrm{fb}^{-1}$ luminosity puts a constraint on the kinetic mixing parameter as $\epsilon_1 \lesssim 0.005$-$0.01$ for the gauge boson mass range of 10-70 GeV. In our model, the $Z_{(B-L)_3}$ boson can be produced via the kinetic mixing[8] and decay into $\mu\bar{\mu}$ via the flavour mixing. The constraint can be interpreted as a bound on $\epsilon_1 s_{\theta_l}^2$, where $s_{\theta_l}^2$ comes from the branching ratio into $\mu\bar{\mu}$. However, this does not give a strong constraint on s_{θ_l} when $\alpha_{(B-L)_3} \lesssim 10^{-4}$. It was also

[7] The $Z_{(B-L)_3}$ boson can also decay into $\mu\bar{\mu}$ via the kinetic mixing with $\mathrm{U}(1)_Y$. Since this process does not dominate for s_{θ_l} satisfying (4.16), we neglect this contribution.

[8] The $Z_{(B-L)_3}$ boson can also be produced from $b\bar{b}$, in which case the constraint can be interpreted as a bound on $f g_{(B-L)_3}/e s_{\theta_l}^2$, where $f = \mathcal{O}(\alpha_s)$, with the quantum chromodynamics fine-structure constant α_s, represents a factor coming from parton distribution functions of b and $\bar{b}$.

JHEP03(2019)021

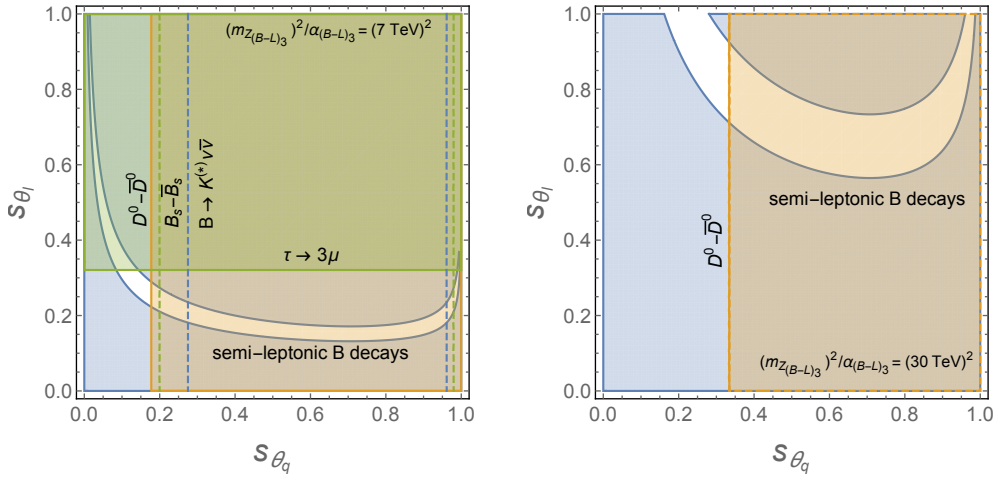

Figure 2. Constraints are summarized in the s_{θ_l}-s_{θ_q} plane, where the shaded region is excluded by the experiments. All the displayed constraints depend only on the combination of $m^2_{Z_{(B-L)_3}}/\alpha_{(B-L)_3}$, which is taken to be $(7\,\mathrm{TeV})^2$ (left panel) and $(30\,\mathrm{TeV})^2$ (right panel).

discussed that the constraint will be improved by a factor about 5 by using $3000\,\mathrm{fb}^{-1}$ of 14 TeV data. In this case, the high-luminosity LHC would observe a dilepton signal for $\alpha_{(B-L)_3} \sim 10^{-4}$.

The $Z_{(B-L)_3}$ boson can also be produced by lepton colliders through the kinetic mixing ϵ_1 and its decay signal can be searched by the future $e\bar{e}$ colliders, such as CEPC [89], ILC [90, 91], and FCC-ee [92]. The relevant process is $e\bar{e} \to \gamma Z_{(B-L)_3}$ followed by $Z_{(B-L)_3} \to \mu\bar{\mu}$. Projected constraints are discussed in ref. [93] in the case where the dark photon couples to the SM particles only via the kinetic mixing with the $\mathrm{U}(1)_Y$ gauge boson. The upper bound on the kinetic mixing parameter was found to be about 0.003. Again, we could interpret their result in the same way as discussed above. The future lepton colliders would observe a signal of $Z_{(B-L)_3}$ boson for $\alpha_{(B-L)_3} \sim 10^{-4}$.

4.3 Summary of the collider constraints

Now we shall put together all the constraints discussed in this section. The result is shown in figure 2, where the shaded regions are excluded by the constraints. Note that all the shown constrains depend on $\alpha_{(B-L)_3}$ and $m_{Z_{(B-L)_3}}$ only via a combination of $m^2_{Z_{(B-L)_3}}/\alpha_{(B-L)_3}$. In the figure, we take $m^2_{Z_{(B-L)_3}}/\alpha_{(B-L)_3} = (7\,\mathrm{TeV})^2$ (left panel) or $(30\,\mathrm{TeV})^2$ (right panel).

We change the value of $m^2_{Z_{(B-L)_3}}/\alpha_{(B-L)_3}$ and find that there is an allowed region when $(3\,\mathrm{TeV})^2 \lesssim m^2_{Z_{(B-L)_3}}/\alpha_{(B-L)_3} \lesssim (49\,\mathrm{TeV})^2$ corresponding to $0.4\,\mathrm{TeV} \lesssim v_{\phi_3} \lesssim 6.9\,\mathrm{TeV}$. This is shown in figure 1 as the green-shaded region. From figure 1, we can see that there is a certain parameter region where we can explain the lepton flavour universality violation in semi-leptonic B decays consistently with the constraints coming from the kinetic mixing. We note that $v_{\phi_3} \ll 2.4\,\mathrm{TeV}$ is required so that N_{R_3} is the subdominant component of DM [see eq. (3.6)]. In particular, all collider constraints as well as the DM constraints can be evaded when $\alpha_{(B-L)_3} = 10^{-4}$, $\alpha_h = 10^{-3}$, $m_{Z_{(B-L)_3}} = 70\,\mathrm{GeV}$, $m_{Z_h} = 10\,\mathrm{MeV}$,

JHEP03(2019)021

$m_\chi = 40\,\mathrm{GeV}$, $\epsilon_1 = 10^{-2}$ and $\epsilon_2 = 4 \times 10^{-2}$, which are used as the reference parameter values throughout this paper.

5 Conclusion

We have proposed a model of DM whose stability is guaranteed by a discrete symmetry. This discrete symmetry is a subgroup of a spontaneously broken hidden $\mathrm{U}(1)_h$ gauge symmetry. The massive gauge boson Z_h is assumed to be much lighter than the DM particle and mediates the velocity-dependent DM self-interaction that are suggested by small-scale issues in structure formation of collisionless cold dark matter. The observed abundance of DM is explained by the thermal relic via the freeze-out mechanism. Motivated by flavoured grand unified theories, we have also introduced right-handed neutrinos and flavoured $B-L$ gauge symmetries. The unwanted relic of Z_h can then decay into neutrinos via the kinetic mixing with the electroweak scale $\mathrm{U}(1)_{(B-L)_3}$ gauge boson $Z_{(B-L)_3}$. This model can also explain the baryon asymmetry of the Universe via the thermal leptogenesis. Furthermore, we have found that this model can explain the lepton flavour universality violation in semi-leptonic B meson decays recently found in LHCb experiment.

Although the hidden sector couples to the SM sector only via the kinetic mixing with the $\mathrm{U}(1)_{(B-L)_3}$ gauge boson, it predicts detectable DM signals in direct detection experiments. Furthermore the subdominant DM annihilation into an electron-positron pair can be examined in indirect detection experiments. Our model predicts a relatively light $\mathrm{U}(1)_{(B-L)_3}$ gauge boson, which leads to interesting signals in collider phenomenology. The $\mathrm{U}(1)_{(B-L)_3}$ gauge boson can be searched by the future high-luminosity LHC experiment and $e\bar{e}$ colliders such as CEPC, ILC, and FCC-ee. These experiments would observe signals when the fine-structure constant for $\mathrm{U}(1)_{(B-L)_3}$ is of order 10^{-4}.

Acknowledgments

A. K. thanks Tae Hyun Jung, Takumi Kuwahara, Chan Beom Park, and Eibun Senaha for useful discussions. A. K. was supported by Institute for Basic Science under the project code, IBS-R018-D1. T. T. Y. was supported in part by the JSPS Grant-in-Aid for Scientific Research No. 26104001, No. 26104009, No. 16H02176, and No. 17H02878, and in part by World Premier International Research Center Initiative (WPI Initiative), MEXT, Japan. T. T. Y. is a Hamamatsu Professor at Kavli IPMU.

A Mixing of gauge bosons

In this appendix, we calculate the mixings among the gauge bosons and interactions induced by the kinetic mixing terms.

The relevant part of the Lagrangian is given by

$$\begin{aligned}\mathcal{L}_{\mathrm{gauge}} = &-\frac{1}{4}F_{Y\,\mu\nu}F_Y^{\mu\nu} - \frac{1}{4}F_{W^3\,\mu\nu}F_{W^3}^{\mu\nu} - \frac{1}{4}F_{(B-L)_3\,\mu\nu}F_{(B-L)_3}^{\mu\nu} - \frac{1}{4}F_{h\,\mu\nu}F_h^{\mu\nu} \\ &-\frac{1}{2}\sin\epsilon_1 F_{Y\,\mu\nu}F_{(B-L)_3}^{\mu\nu} - \frac{1}{2}\cos\epsilon_1 \sin\epsilon_2 F_{(B-L)_3\,\mu\nu}F_h^{\mu\nu} - \frac{1}{2}V_\mu^{\mathrm{T}} M_V^2 V^\mu\,,\end{aligned} \tag{A.1}$$

where we have replaced ϵ_1 and ϵ_2 by $\sin\epsilon_1$ ($\simeq \epsilon_1$ for $\epsilon_1 \ll 1$) and $\cos\epsilon_1 \sin\epsilon_2$ ($\simeq \epsilon_2$ for $\epsilon_1, \epsilon_2 \ll 1$) for convenience. Here $F_{W^3\,\mu\nu}$ is the field strength of the Cartan subgroup of weak SU(2). We have defined $V^\mu = (B^\mu, W^{3\,\mu}, Z^\mu_{(B-L)_3}, Z^\mu_h)^{\mathrm{T}}$ with B^μ and $W^{3\,\mu}$ being the gauge bosons of $\mathrm{U}(1)_Y$ and the Cartan subgroup of weak SU(2), respectively. The mass squared matrix is given by

$$M_V^2 = \begin{pmatrix} m_Z^2 s_W^2 & -m_Z^2 c_W s_W & 0 & 0 \\ -m_Z^2 c_W s_W & m_Z^2 c_W^2 & 0 & 0 \\ 0 & 0 & m^2_{Z_{(B-L)_3}} & 0 \\ 0 & 0 & 0 & m^2_{Z_h} \end{pmatrix}, \tag{A.2}$$

where $m_Z = m_{W^\pm}/c_W$, $c_W \equiv \cos\theta_W$, and $s_W \equiv \sin\theta_W$ with $m_{W^\pm}$ and θ_W being the W boson mass and Weinberg angle, respectively.

First, we diagonalize the kinetic terms and isolate the massless gauge boson A^μ by

$$\begin{pmatrix} B^\mu \\ W^{3\,\mu} \\ Z^\mu_{(B-L)_3} \\ Z^\mu_h \end{pmatrix} = \begin{pmatrix} 1 & 0 & -t_{\epsilon_1}/c_{\epsilon_2} & 0 \\ 0 & 1 & 0 & 0 \\ 0 & 0 & 1/(c_{\epsilon_1} c_{\epsilon_2}) & 0 \\ 0 & 0 & -t_{\epsilon_2} & 1 \end{pmatrix} \begin{pmatrix} c_W & -s_W & 0 & 0 \\ s_W & c_W & 0 & 0 \\ 0 & 0 & 1 & 0 \\ 0 & 0 & 0 & 1 \end{pmatrix} \begin{pmatrix} A^\mu \\ \tilde{Z}_1^\mu \\ \tilde{Z}_2^\mu \\ \tilde{Z}_3^\mu \end{pmatrix}, \tag{A.3}$$

where $t_{\epsilon_i} \equiv \tan\epsilon_i$ and $c_{\epsilon_i} \equiv \cos\epsilon_i$ ($i = 1, 2$). In terms of this basis, the mass squared matrix for $(\tilde{Z}_1^\mu, \tilde{Z}_2^\mu, \tilde{Z}_3^\mu)$ is given by $\tilde{M}_V^2$, where

$$(\tilde{M}_V^2)_{11} = m_Z^2\,, \tag{A.4}$$
$$(\tilde{M}_V^2)_{12} = m_Z^2 s_W t_{\epsilon_1}/c_{\epsilon_2}\,, \tag{A.5}$$
$$(\tilde{M}_V^2)_{13} = 0\,, \tag{A.6}$$
$$(\tilde{M}_V^2)_{22} = m^2_{Z_{(B-L)_3}}/(c^2_{\epsilon_1} c^2_{\epsilon_2}) + m_Z^2 s_W^2 t^2_{\epsilon_1}/c^2_{\epsilon_2} + m^2_{Z_h} t^2_{\epsilon_2}\,, \tag{A.7}$$
$$(\tilde{M}_V^2)_{23} = -m^2_{Z_h} t_{\epsilon_2}\,, \tag{A.8}$$
$$(\tilde{M}_V^2)_{33} = m^2_{Z_h}\,. \tag{A.9}$$

Second, we diagonalize the mass squared matrix by rotating the vector fields as

$$\begin{pmatrix} A^\mu \\ \tilde{Z}_1^\mu \\ \tilde{Z}_2^\mu \\ \tilde{Z}_3^\mu \end{pmatrix} = R_{12}(\xi_1) R_{32}(\xi_2) R_{31}(\xi_3) \begin{pmatrix} A^\mu \\ Z_1^\mu \\ Z_2^\mu \\ Z_3^\mu \end{pmatrix}, \tag{A.10}$$

JHEP03(2019)021

where $R_{ij}(\xi)$ is the rotation matrix for $(Z_i^\mu, Z_j^\mu)^{\rm T}$ $(i,j=1,2,3)$ by an angle ξ:

$$R_{12}(\xi_1) = \begin{pmatrix} 1 & 0 & 0 & 0 \\ 0 & c_{\xi_1} & -s_{\xi_1} & 0 \\ 0 & s_{\xi_1} & c_{\xi_1} & 0 \\ 0 & 0 & 0 & 1 \end{pmatrix}, \tag{A.11}$$

$$R_{32}(\xi_2) = \begin{pmatrix} 1 & 0 & 0 & 0 \\ 0 & 1 & 0 & 0 \\ 0 & 0 & c_{\xi_2} & s_{\xi_2} \\ 0 & 0 & -s_{\xi_2} & c_{\xi_2} \end{pmatrix}, \tag{A.12}$$

$$R_{31}(\xi_3) = \begin{pmatrix} 1 & 0 & 0 & 0 \\ 0 & c_{\xi_3} & 0 & s_{\xi_3} \\ 0 & 0 & 1 & 0 \\ 0 & -s_{\xi_3} & 0 & c_{\xi_3} \end{pmatrix}. \tag{A.13}$$

In this paper, we are interested in the case where $\epsilon_i \ll 1$ and $m_{Z_h} \ll m_{Z_{(B-L)_3}}, m_Z$. In this case, we can approximate the rotation angles as

$$\tan 2\xi_1 \simeq \frac{2(\tilde{M}_V^2)_{12}}{(\tilde{M}_V^2)_{11} - (\tilde{M}_V^2)_{22}} \simeq \frac{2 s_W \epsilon_1 m_Z^2}{m_Z^2 - m_{Z_{(B-L)_3}}^2}, \tag{A.14}$$

$$\xi_2 \simeq \frac{(\tilde{M}_V^2)_{23} c_{\xi_1}}{(\tilde{M}_V^2)_{33} - m_{Z_2'}^2} \simeq c_{\xi_1} \epsilon_2 \frac{m_{Z_h}^2}{m_{Z_2'}^2}, \tag{A.15}$$

$$\xi_3 \simeq \frac{(\tilde{M}_V^2)_{23} s_{\xi_1} c_{\xi_2}}{(\tilde{M}_V^2)_{33} - m_{Z_1}^2} \simeq s_{\xi_1} \epsilon_2 \frac{m_{Z_h}^2}{m_{Z_1}^2}, \tag{A.16}$$

and the mass eigenvalues as

$$m_{Z_1}^2 \simeq \frac{m_Z^2 - m_{Z_2'}^2 s_{\xi_1}^2}{c_{\xi_1}^2}, \tag{A.17}$$

$$m_{Z_2}^2 \simeq m_{Z_2'}^2 \simeq c_{\xi_1}^2 m_{Z_{(B-L)_3}}^2 + s_{\xi_1}^2 m_Z^2 \left(1 - \frac{2 s_W \epsilon_1}{t_{\xi_1}}\right), \tag{A.18}$$

$$m_{Z_3}^2 \simeq m_{Z_h}^2, \tag{A.19}$$

in the leading order for ϵ_i and $m_{Z_h}/m_{Z_{(B-L)_3}}$, where we have defined[9]

$$m_{Z_2'}^2 = c_{\xi_1}^2 (\tilde{M}_V^2)_{22} + s_{\xi_1}^2 m_Z^2 \left(1 - \frac{2(\tilde{M}_V)_{12}^2}{t_{\xi_1} m_Z^2}\right). \tag{A.20}$$

[9]There are some typos in the literature in the context of kinetic mixing between $\mathrm{U}(1)_Y$ and $\mathrm{U}(1)'$. In ref. [94], the sign of the rotation angle ζ in eq. (B-5) is opposite to the one used in the main text. In ref. [95], where they cite ref. [94], the sign in the parenthesis in eq. (9) should be opposite.

JHEP03(2019)021

In the main text of this paper, we simply denote the physical masses by m_Z, $m_{Z_{(B-L)_3}}$, and m_{Z_h}, noting $\xi_1 \simeq s_W\epsilon_1/(1-(m_{Z_{(B-L)_3}}/m_Z)^2) \ll 1$ in most of the parameter space that we are interested in.

The current interactions are given by

$$\mathcal{L}_{\rm int} = (V^\mu)^{\rm T}\tilde{J}_\mu = (V^\mu_{\rm mass})^{\rm T}\mathcal{M}J_\mu\,, \tag{A.21}$$

where $V^\mu_{\rm mass} = (A^\mu, Z_1^\mu, Z_2^\mu, Z_3^\mu)^{\rm T}$,

$$J^\mu \equiv \begin{pmatrix} eJ^\mu_{\rm EM} \\ g/c_W J^\mu_{\rm Z^0} \\ g_{(B-L)_3}J^\mu_{(B-L)_3} \\ g_h J^\mu_h \end{pmatrix} \equiv \begin{pmatrix} c_W & s_W & 0 & 0 \\ -s_W & c_W & 0 & 0 \\ 0 & 0 & 1 & 0 \\ 0 & 0 & 0 & 1 \end{pmatrix} \tilde{J}^\mu\,, \tag{A.22}$$

and

$$\mathcal{M} = R^{\rm T}_{31}(\xi_3)R^{\rm T}_{32}(\xi_2)R^{\rm T}_{12}(\xi_1) \begin{pmatrix} 1 & 0 & 0 & 0 \\ 0 & 1 & 0 & 0 \\ -c_W t_{\epsilon_1}/c_{\epsilon_2} & s_W t_{\epsilon_1}/c_{\epsilon_2} & 1/(c_{\epsilon_1}c_{\epsilon_2}) & -t_{\epsilon_2} \\ 0 & 0 & 0 & 1 \end{pmatrix} \tag{A.23}$$

$$\simeq \begin{pmatrix} 1 & 0 & 0 & 0 \\ -c_W\epsilon_1 s_{\xi_1} & s_W\epsilon_1 s_{\xi_1} + c_{\xi_1} & s_{\xi_1} & -\epsilon_2 s_{\xi_1} - \xi_3 \\ -c_W\epsilon_1 c_{\xi_1} & s_W\epsilon_1 c_{\xi_1} - s_{\xi_1} & c_{\xi_1} & -\epsilon_2 c_{\xi_1} - \xi_2 \\ -c_W\epsilon_1(c_{\xi_1}\xi_2 + s_{\xi_1}\xi_3) & s_W\epsilon_1(c_{\xi_1}\xi_2 + s_{\xi_1}\xi_3) - s_{\xi_1}\xi_2 + c_{\xi_1}\xi_3 & c_{\xi_1}\xi_2 + s_{\xi_1}\xi_3 & 1 \end{pmatrix}. \tag{A.24}$$

Integrating out Z_i $(i = 1, 2, 3)$, one can check that the effective interactions between J^μ_h and $J^\mu_{\rm EM}$ or $J^\mu_{Z^0}$ are suppressed by a factor of order $g_h e\xi_1\xi_2/m^2_{Z_2} \simeq g_h e\epsilon_1\epsilon_2 m^2_{Z_h}/m^4_{Z_{(B-L)_3}}$. This implies that the leading-order interaction term, which is suppressed only by $g_h e c_W\epsilon_1\epsilon_2/m^2_{Z_{(B-L)_3}}$, is cancelled in a large m_{Z_3} limit. However, the momentum transfer for the process that we are interested in is of order m_{Z_3}. Thus we expect that the leading-order interaction is not completely cancelled out but is suppressed by a factor of $q^2/(q^2 + m^2_{Z_3})$, where q^2 is the square of the momentum transfer.

B Phase transition and thermal inflation

In this appendix, we comment on the effects of the phase transition from the SSB of $\mathrm{U}(1)_h$, in which the dark Higgs boson Ψ develops the VEV v_Ψ.[10]

Since it breaks the local Abelian gauge symmetry, cosmic strings form through the phase transition. However, their effects are negligible in our model because the energy

[10] We do not discuss the phase transitions of the $\mathrm{U}(1)_{(B-L)_i}$ breaking fields Φ_i because their potentials may be complicated by additional scalars and heavy fermions that are required to reproduce the proper Yukawa structure (see, e.g., ref. [20]).

JHEP03(2019)021

density of cosmic strings is suppressed by a factor of the VEV squared in the Planck units when compared to the total energy density of the Universe.

If the VEV of a scalar field is much larger than its (zero temperature + thermal) mass, the potential energy before the phase transition may be much larger than the energy of the thermal plasma. In this case, the energy density of the Universe becomes dominated by the former vacuum energy and a mini inflation called a thermal inflation occurs through the phase transition [96, 97]. The duration of the thermal inflation depends on the ratio between the VEV and (zero temperature + thermal) mass of the SSB field. After the thermal inflation, the vacuum energy will be released into the radiation and the entropy production proceeds. As a result, the baryon asymmetry is diluted due to the entropy production at the time of this reheating.

Here, we give a quantitative estimate of the dilution of the thermal relic through the entropy production. The (zero temperature + thermal) potential of Ψ is given by

$$V(\Psi) = \lambda \left(|\Psi|^2 - \frac{1}{2} v_\psi^2 \right)^2 + V_T(\Psi) \,, \tag{B.1}$$

where λ is a quartic coupling. The mass of ψ at the vacuum is given by $\sqrt{2\lambda}\, v_\psi$. The thermal potential V_T from ψ and Z_h is approximately given by

$$V_T(\Psi) = \left(\frac{\lambda}{3} + q_\psi^2 \frac{g_h^2}{4} \right) T^2 \, |\Psi|^2 \,, \tag{B.2}$$

where q_ψ $(= 3)$ is the charge of Ψ. At a high temperature, the thermal potential dominates and Ψ is stabilized at $\Psi = 0$. When the temperature becomes lower than the critical temperature T_c, which is given by

$$T_c = \sqrt{\frac{\lambda}{\lambda/3 + q_\psi^2 g_h^2/4}}\, v_\psi \,, \tag{B.3}$$

the potential becomes unstable at $\Psi = 0$ and the scalar field starts to oscillate around the true vacuum at $\Psi = v_\psi/\sqrt{2}$. We define a dilution factor as the ratio of the initial to the final comoving entropy density as

$$\Delta \equiv \frac{s_f a_f^3}{s_i a_i^3} = 1 + \frac{4}{3} \frac{g_{*s}(T_{\mathrm{RH},\psi})}{g_*(T_{\mathrm{RH},\psi})\, T_{\mathrm{RH},\psi}} \frac{V(0)}{(2\pi^2/45)\, g_{*s}(T_c)\, T_c^3} \,, \tag{B.4}$$

where (I) a_i (a_f) is the scale factor, s_i (s_f) is the entropy density before (after) the thermal inflation; (II) $V(0) = \lambda v_\psi^4/4$; and (III) g_{*s} (g_*) is the effective number of relativistic degrees of freedom for the entropy (energy) density as a function of T. The reheating temperature of oscillating ψ satisfies $T_{\mathrm{RH},\psi} < [30V(0)/\{g_*(T_{\mathrm{RH},\psi})\, \pi^2\}]^{1/4}$. To avoid the washout effect due to the thermal inflation, we require $\Delta \approx 1$ corresponding to

$$\left(\frac{m_{Z_h}^2}{m_h^2} + \frac{2}{3} \right) \lesssim \lambda^{-1/2} \left(\frac{4\sqrt{2}\pi^2\, g_{*s}(T_c)\, g_*(T_{\mathrm{RH},\psi})}{15\, g_{*s}(T_{\mathrm{RH},\psi})} \right)^{2/3} \left(\frac{15}{2\pi^2 g_*(T_{\mathrm{RH},\psi})} \right)^{1/6} . \tag{B.5}$$

It follows that the gauge boson mass cannot be arbitrary larger than the mass of the SSB field. This condition is easily satisfied in our model although it is non-trivial in other models with hierarchical mass scales.

JHEP03(2019)021

References

[1] S. Tulin and H.-B. Yu, *Dark matter self-interactions and small scale structure*, *Phys. Rept.* **730** (2018) 1 [arXiv:1705.02358] [INSPIRE].

[2] J.S. Bullock and M. Boylan-Kolchin, *Small-scale challenges to the ΛCDM paradigm*, *Ann. Rev. Astron. Astrophys.* **55** (2017) 343 [arXiv:1707.04256] [INSPIRE].

[3] M. Kaplinghat, S. Tulin and H.-B. Yu, *Dark matter halos as particle colliders: unified solution to small-scale structure puzzles from dwarfs to clusters*, *Phys. Rev. Lett.* **116** (2016) 041302 [arXiv:1508.03339] [INSPIRE].

[4] A. Kamada, M. Kaplinghat, A.B. Pace and H.-B. Yu, *Self-interacting dark matter can explain diverse galactic rotation curves*, *Phys. Rev. Lett.* **119** (2017) 111102 [arXiv:1611.02716] [INSPIRE].

[5] P. Creasey, O. Sameie, L.V. Sales, H.-B. Yu, M. Vogelsberger and J. Zavala, *Spreading out and staying sharp — creating diverse rotation curves via baryonic and self-interaction effects*, *Mon. Not. Roy. Astron. Soc.* **468** (2017) 2283 [arXiv:1612.03903] [INSPIRE].

[6] T. Ren, A. Kwa, M. Kaplinghat and H.-B. Yu, *Reconciling the diversity and uniformity of galactic rotation curves with self-interacting dark matter*, arXiv:1808.05695 [INSPIRE].

[7] K.A. Oman et al., *The unexpected diversity of dwarf galaxy rotation curves*, *Mon. Not. Roy. Astron. Soc.* **452** (2015) 3650 [arXiv:1504.01437] [INSPIRE].

[8] A.B. Newman, T. Treu, R.S. Ellis and D.J. Sand, *The density profiles of massive, relaxed galaxy clusters. II. Separating luminous and dark matter in cluster cores*, *Astrophys. J.* **765** (2013) 25 [arXiv:1209.1392] [INSPIRE].

[9] T. Bringmann, F. Kahlhoefer, K. Schmidt-Hoberg and P. Walia, *Strong constraints on self-interacting dark matter with light mediators*, *Phys. Rev. Lett.* **118** (2017) 141802 [arXiv:1612.00845] [INSPIRE].

[10] A. Kamada, K. Kaneta, K. Yanagi and H.-B. Yu, *Self-interacting dark matter and muon $g-2$ in a gauged $\mathrm{U}(1)_{L_\mu - L_\tau}$ model*, *JHEP* **06** (2018) 117 [arXiv:1805.00651] [INSPIRE].

[11] J.L. Feng, M. Kaplinghat, H. Tu and H.-B. Yu, *Hidden charged dark matter*, *JCAP* **07** (2009) 004 [arXiv:0905.3039] [INSPIRE].

[12] S. Tulin, H.-B. Yu and K.M. Zurek, *Resonant dark forces and small-scale structure*, *Phys. Rev. Lett.* **110** (2013) 111301 [arXiv:1210.0900] [INSPIRE].

[13] B. Dasgupta and J. Kopp, *Cosmologically safe eV-scale sterile neutrinos and improved dark matter structure*, *Phys. Rev. Lett.* **112** (2014) 031803 [arXiv:1310.6337] [INSPIRE].

[14] T. Bringmann, J. Hasenkamp and J. Kersten, *Tight bonds between sterile neutrinos and dark matter*, *JCAP* **07** (2014) 042 [arXiv:1312.4947] [INSPIRE].

[15] P. Ko and Y. Tang, *νΛMDM: a model for sterile neutrino and dark matter reconciles cosmological and neutrino oscillation data after BICEP2*, *Phys. Lett.* **B 739** (2014) 62 [arXiv:1404.0236] [INSPIRE].

JHEP03(2019)021

[16] J.F. Cherry, A. Friedland and I.M. Shoemaker, *Neutrino portal dark matter: from dwarf galaxies to IceCube*, arXiv:1411.1071 [INSPIRE].

[17] T. Kitahara and Y. Yamamoto, *Protophobic light vector boson as a mediator to the dark sector*, *Phys. Rev.* **D 95** (2017) 015008 [arXiv:1609.01605] [INSPIRE].

[18] E. Ma, *Inception of self-interacting dark matter with dark charge conjugation symmetry*, *Phys. Lett.* **B 772** (2017) 442 [arXiv:1704.04666] [INSPIRE].

[19] O. Balducci, S. Hofmann and A. Kassiteridis, *Flavor structures in the dark Standard Model TeV-paradigm*, arXiv:1810.07198 [INSPIRE].

[20] R. Alonso, P. Cox, C. Han and T.T. Yanagida, *Flavoured B-L local symmetry and anomalous rare B decays*, *Phys. Lett.* **B 774** (2017) 643 [arXiv:1705.03858] [INSPIRE].

[21] K.S. Babu, S.M. Barr and I. Gogoladze, *Family unification with* SO(10), *Phys. Lett.* **B 661** (2008) 124 [arXiv:0709.3491] [INSPIRE].

[22] P. Minkowski, $\mu \to e\gamma$ *at a rate of one out of* 10^9 *muon decays?*, *Phys. Lett.* **B 67** (1977) 421 [INSPIRE].

[23] T. Yanagida, *Horizontal gauge symmetry and masses of neutrinos*, *Conf. Proc.* **C 7902131** (1979) 95 [INSPIRE].

[24] M. Gell-Mann, P. Ramond and R. Slansky, *Complex spinors and unified theories*, *Conf. Proc.* **C 790927** (1979) 315 [arXiv:1306.4669] [INSPIRE].

[25] S.L. Glashow, *The future of elementary particle physics*, *NATO Sci. Ser.* **B 61** (1980) 687 [INSPIRE].

[26] M. Fukugita and T. Yanagida, *Baryogenesis without grand unification*, *Phys. Lett.* **B 174** (1986) 45 [INSPIRE].

[27] W. Buchmüller, P. Di Bari and M. Plümacher, *Cosmic microwave background, matter-antimatter asymmetry and neutrino masses*, *Nucl. Phys.* **B 643** (2002) 367 [*Erratum ibid.* **B 793** (2008) 362] [hep-ph/0205349] [INSPIRE].

[28] G.F. Giudice, A. Notari, M. Raidal, A. Riotto and A. Strumia, *Towards a complete theory of thermal leptogenesis in the SM and MSSM*, *Nucl. Phys.* **B 685** (2004) 89 [hep-ph/0310123] [INSPIRE].

[29] W. Buchmüller, R.D. Peccei and T. Yanagida, *Leptogenesis as the origin of matter*, *Ann. Rev. Nucl. Part. Sci.* **55** (2005) 311 [hep-ph/0502169] [INSPIRE].

[30] S. Davidson, E. Nardi and Y. Nir, *Leptogenesis*, *Phys. Rept.* **466** (2008) 105 [arXiv:0802.2962] [INSPIRE].

[31] P. Cox, C. Han and T.T. Yanagida, *Right-handed neutrino dark matter in a* U(1) *extension of the Standard Model*, *JCAP* **01** (2018) 029 [arXiv:1710.01585] [INSPIRE].

[32] LHCb collaboration, *Test of lepton universality using* $B^+ \to K^+\ell^+\ell^-$ *decays*, *Phys. Rev. Lett.* **113** (2014) 151601 [arXiv:1406.6482] [INSPIRE].

[33] LHCb collaboration, *Test of lepton universality with* $B^0 \to K^{*0}\ell^+\ell^-$ *decays*, *JHEP* **08** (2017) 055 [arXiv:1705.05802] [INSPIRE].

[34] L. Bian, S.-M. Choi, Y.-J. Kang and H.M. Lee, *Minimal flavored* $\mathrm{U}(1)'$ *for B-meson anomalies*, *Phys. Rev.* **D 96** (2017) 075038 [arXiv:1707.04811] [INSPIRE].

JHEP03(2019)021

[35] P.S.B. Dev, R.N. Mohapatra and Y. Zhang, *Leptogenesis constraints on B-L breaking Higgs boson in TeV scale seesaw models*, *JHEP* **03** (2018) 122 [arXiv:1711.07634] [INSPIRE].

[36] G.H. Duan, X. Fan, M. Frank, C. Han and J.M. Yang, *A minimal* U(1)′ *extension of MSSM in light of the B decay anomaly*, *Phys. Lett.* **B 789** (2019) 54 [arXiv:1808.04116] [INSPIRE].

[37] M. Duerr, K. Schmidt-Hoberg and S. Wild, *Self-interacting dark matter with a stable vector mediator*, *JCAP* **09** (2018) 033 [arXiv:1804.10385] [INSPIRE].

[38] T. Binder, M. Gustafsson, A. Kamada, S.M.R. Sandner and M. Wiesner, *Reannihilation of self-interacting dark matter*, *Phys. Rev.* **D 97** (2018) 123004 [arXiv:1712.01246] [INSPIRE].

[39] S. Tulin, H.-B. Yu and K.M. Zurek, *Beyond collisionless dark matter: particle physics dynamics for dark matter halo structure*, *Phys. Rev.* **D 87** (2013) 115007 [arXiv:1302.3898] [INSPIRE].

[40] F. Kahlhoefer, K. Schmidt-Hoberg, M.T. Frandsen and S. Sarkar, *Colliding clusters and dark matter self-interactions*, *Mon. Not. Roy. Astron. Soc.* **437** (2014) 2865 [arXiv:1308.3419] [INSPIRE].

[41] F. Kahlhoefer, K. Schmidt-Hoberg and S. Wild, *Dark matter self-interactions from a general spin-0 mediator*, *JCAP* **08** (2017) 003 [arXiv:1704.02149] [INSPIRE].

[42] J.L. Feng, M. Kaplinghat and H.-B. Yu, *Halo-shape and relic-density exclusions of Sommerfeld-enhanced dark matter explanations of cosmic ray excesses*, *Phys. Rev. Lett.* **104** (2010) 151301 [arXiv:0911.0422] [INSPIRE].

[43] S.A. Khrapak, A.V. Ivlev, G.E. Morfill and S.K. Zhdanov, *Scattering in the attractive Yukawa potential in the limit of strong interaction*, *Phys. Rev. Lett.* **90** (2003) 225002 [INSPIRE].

[44] F.-Y. Cyr-Racine, K. Sigurdson, J. Zavala, T. Bringmann, M. Vogelsberger and C. Pfrommer, *ETHOS — an effective theory of structure formation: from dark particle physics to the matter distribution of the universe*, *Phys. Rev.* **D 93** (2016) 123527 [arXiv:1512.05344] [INSPIRE].

[45] A. Kamada and H.-B. Yu, *Coherent propagation of PeV neutrinos and the dip in the neutrino spectrum at IceCube*, *Phys. Rev.* **D 92** (2015) 113004 [arXiv:1504.00711] [INSPIRE].

[46] V. Poulin, J. Lesgourgues and P.D. Serpico, *Cosmological constraints on exotic injection of electromagnetic energy*, *JCAP* **03** (2017) 043 [arXiv:1610.10051] [INSPIRE].

[47] M. Hufnagel, K. Schmidt-Hoberg and S. Wild, *BBN constraints on MeV-scale dark sectors. Part II: electromagnetic decays*, *JCAP* **11** (2018) 032 [arXiv:1808.09324] [INSPIRE].

[48] A.L. Fitzpatrick, D. Hooper and K.M. Zurek, *Implications of CoGeNT and DAMA for light WIMP dark matter*, *Phys. Rev.* **D 81** (2010) 115005 [arXiv:1003.0014] [INSPIRE].

[49] XENON collaboration, *Dark matter search results from a one ton-year exposure of XENON1T*, *Phys. Rev. Lett.* **121** (2018) 111302 [arXiv:1805.12562] [INSPIRE].

[50] XENON collaboration, *Physics reach of the XENON1T dark matter experiment*, *JCAP* **04** (2016) 027 [arXiv:1512.07501] [INSPIRE].

[51] DarkSide collaboration, *DarkSide-20k: a 20 tonne two-phase LAr TPC for direct dark matter detection at LNGS*, *Eur. Phys. J. Plus* **133** (2018) 131 [arXiv:1707.08145] [INSPIRE].

JHEP03(2019)021

[52] LUX-ZEPLIN (LZ) collaboration, *LUX-ZEPLIN (LZ) technical design report*, arXiv:1703.09144 [INSPIRE].

[53] DARWIN collaboration, *DARWIN: towards the ultimate dark matter detector*, *JCAP* **11** (2016) 017 [arXiv:1606.07001] [INSPIRE].

[54] SUPER-KAMIOKANDE collaboration, *Searching for dark matter annihilation into neutrinos with Super-Kamiokande*, in *Proceedings, Meeting of the APS Division of Particles and Fields (DPF 2015)*, Ann Arbor, MI, U.S.A., 4–8 August 2015 [arXiv:1510.07999] [INSPIRE].

[55] R.K. Leane, T.R. Slatyer, J.F. Beacom and K.C.Y. Ng, *GeV-scale thermal WIMPs: not even slightly ruled out*, *Phys. Rev.* **D 98** (2018) 023016 [arXiv:1805.10305] [INSPIRE].

[56] J.L. Feng, M. Kaplinghat and H.-B. Yu, *Sommerfeld enhancements for thermal relic dark matter*, *Phys. Rev.* **D 82** (2010) 083525 [arXiv:1005.4678] [INSPIRE].

[57] BABAR collaboration, *Test of lepton universality in $\Upsilon(1S)$ decays at BaBar*, *Phys. Rev. Lett.* **104** (2010) 191801 [arXiv:1002.4358] [INSPIRE].

[58] ATLAS collaboration, *Search for additional heavy neutral Higgs and gauge bosons in the ditau final state produced in 36 fb^{-1} of pp collisions at $\sqrt{s} = 13$ TeV with the ATLAS detector*, *JHEP* **01** (2018) 055 [arXiv:1709.07242] [INSPIRE].

[59] CMS collaboration, *Search for low mass vector resonances decaying into quark-antiquark pairs in proton-proton collisions at $\sqrt{s} = 13$ TeV*, *JHEP* **01** (2018) 097 [arXiv:1710.00159] [INSPIRE].

[60] ATLAS collaboration, *Search for light resonances decaying to boosted quark pairs and produced in association with a photon or a jet in proton-proton collisions at $\sqrt{s} = 13$ TeV with the ATLAS detector*, *Phys. Lett.* **B 788** (2019) 316 [arXiv:1801.08769] [INSPIRE].

[61] PARTICLE DATA GROUP collaboration, *Review of particle physics*, *Phys. Rev.* **D 98** (2018) 030001 [INSPIRE].

[62] W. Altmannshofer, P. Stangl and D.M. Straub, *Interpreting hints for lepton flavor universality violation*, *Phys. Rev.* **D 96** (2017) 055008 [arXiv:1704.05435] [INSPIRE].

[63] G. D'Amico et al., *Flavour anomalies after the R_{K^*} measurement*, *JHEP* **09** (2017) 010 [arXiv:1704.05438] [INSPIRE].

[64] B. Capdevila, A. Crivellin, S. Descotes-Genon, J. Matias and J. Virto, *Patterns of new physics in $b \to s\ell^+\ell^-$ transitions in the light of recent data*, *JHEP* **01** (2018) 093 [arXiv:1704.05340] [INSPIRE].

[65] G. Hiller and I. Nišandžić, *R_K and R_{K^*} beyond the Standard Model*, *Phys. Rev.* **D 96** (2017) 035003 [arXiv:1704.05444] [INSPIRE].

[66] M. Ciuchini et al., *On flavourful easter eggs for new physics hunger and lepton flavour universality violation*, *Eur. Phys. J.* **C 77** (2017) 688 [arXiv:1704.05447] [INSPIRE].

[67] L.-S. Geng, B. Grinstein, S. Jäger, J. Martin Camalich, X.-L. Ren and R.-X. Shi, *Towards the discovery of new physics with lepton-universality ratios of $b \to s\ell\ell$ decays*, *Phys. Rev.* **D 96** (2017) 093006 [arXiv:1704.05446] [INSPIRE].

[68] A.K. Alok, B. Bhattacharya, A. Datta, D. Kumar, J. Kumar and D. London, *New physics in $b \to s\mu^+\mu^-$ after the measurement of R_{K^*}*, *Phys. Rev.* **D 96** (2017) 095009 [arXiv:1704.07397] [INSPIRE].

JHEP03(2019)021

[69] CMS and LHCb collaborations, *Observation of the rare $B_s^0 \to \mu^+\mu^-$ decay from the combined analysis of CMS and LHCb data*, *Nature* **522** (2015) 68 [arXiv:1411.4413] [INSPIRE].

[70] A.J. Buras, J. Girrbach-Noe, C. Niehoff and D.M. Straub, *$B \to K^{(*)}\nu\bar{\nu}$ decays in the Standard Model and beyond*, *JHEP* **02** (2015) 184 [arXiv:1409.4557] [INSPIRE].

[71] BELLE collaboration, *Search for $B \to h^{(*)}\nu\bar{\nu}$ with the full Belle $\Upsilon(4S)$ data sample*, *Phys. Rev.* **D 87** (2013) 111103 [arXiv:1303.3719] [INSPIRE].

[72] BABAR collaboration, *Search for $B \to K^{(*)}\nu\bar{\nu}$ and invisible quarkonium decays*, *Phys. Rev.* **D 87** (2013) 112005 [arXiv:1303.7465] [INSPIRE].

[73] M. Ciuchini, E. Franco, V. Lubicz, G. Martinelli, I. Scimemi and L. Silvestrini, *Next-to-leading order QCD corrections to $\Delta F = 2$ effective Hamiltonians*, *Nucl. Phys.* **B 523** (1998) 501 [hep-ph/9711402] [INSPIRE].

[74] A.J. Buras, M. Misiak and J. Urban, *Two-loop QCD anomalous dimensions of flavor-changing four-quark operators within and beyond the Standard Model*, *Nucl. Phys.* **B 586** (2000) 397 [hep-ph/0005183] [INSPIRE].

[75] T. Inami and C.S. Lim, *Effects of superheavy quarks and leptons in low-energy weak processes $KL \to \mu\bar{\mu}$, $K^+ \to \pi^+\nu\nu$ and $K^0 \leftrightarrow \bar{K}^0$*, *Prog. Theor. Phys.* **65** (1981) 297 [*Erratum ibid.* **65** (1981) 1772] [INSPIRE].

[76] A.J. Buras, M. Jamin and P.H. Weisz, *Leading and next-to-leading QCD corrections to ϵ-parameter and B^0-$\bar{B}^0$ mixing in the presence of a heavy top quark*, *Nucl. Phys.* **B 347** (1990) 491 [INSPIRE].

[77] A. Lenz et al., *Anatomy of new physics in B-$\bar{B}$ mixing*, *Phys. Rev.* **D 83** (2011) 036004 [arXiv:1008.1593] [INSPIRE].

[78] UTFIT collaboration, *Model-independent constraints on $\Delta F = 2$ operators and the scale of new physics*, *JHEP* **03** (2008) 049 [arXiv:0707.0636] [INSPIRE].

[79] ETM collaboration, *Leptonic decay constants f_K, f_D, and f_{D_s} with $N_f = 2 + 1 + 1$ twisted-mass lattice QCD*, *Phys. Rev.* **D 91** (2015) 054507 [arXiv:1411.7908] [INSPIRE].

[80] ETM collaboration, *$\Delta S = 2$ and $\Delta C = 2$ bag parameters in the Standard Model and beyond from $N_f = 2 + 1 + 1$ twisted-mass lattice QCD*, *Phys. Rev.* **D 92** (2015) 034516 [arXiv:1505.06639] [INSPIRE].

[81] E. Golowich, J. Hewett, S. Pakvasa and A.A. Petrov, *Implications of D^0-$\bar{D}^0$ mixing for new physics*, *Phys. Rev.* **D 76** (2007) 095009 [arXiv:0705.3650] [INSPIRE].

[82] HFLAV collaboration, *Averages of b-hadron, c-hadron and τ-lepton properties as of summer 2016*, *Eur. Phys. J.* **C 77** (2017) 895 [arXiv:1612.07233] [INSPIRE].

[83] BELLE collaboration, *Search for lepton flavor violating τ decays into three leptons with 719 million produced $\tau^+\tau^-$ pairs*, *Phys. Lett.* **B 687** (2010) 139 [arXiv:1001.3221] [INSPIRE].

[84] ATLAS collaboration, *Search for new high-mass phenomena in the dilepton final state using 36 fb^{-1} of proton-proton collision data at $\sqrt{s} = 13$ TeV with the ATLAS detector*, *JHEP* **10** (2017) 182 [arXiv:1707.02424] [INSPIRE].

[85] ATLAS collaboration, *Search for lepton-flavor violation in different-flavor, high-mass final states in pp collisions at $\sqrt{s} = 13$ TeV with the ATLAS detector*, *Phys. Rev.* **D 98** (2018) 092008 [arXiv:1807.06573] [INSPIRE].

JHEP03(2019)021

[86] ATLAS collaboration, *Measurements of four-lepton production at the Z resonance in pp collisions at $\sqrt{s} = 7$ and 8 TeV with ATLAS*, *Phys. Rev. Lett.* **112** (2014) 231806 [arXiv:1403.5657] [INSPIRE].

[87] C. Bonilla, T. Modak, R. Srivastava and J.W.F. Valle, $U(1)_{B_3-3L_\mu}$ *gauge symmetry as a simple description of* $b \to s$ *anomalies*, *Phys. Rev.* **D 98** (2018) 095002 [arXiv:1705.00915] [INSPIRE].

[88] I. Hoenig, G. Samach and D. Tucker-Smith, *Searching for dilepton resonances below the Z mass at the LHC*, *Phys. Rev.* **D 90** (2014) 075016 [arXiv:1408.1075] [INSPIRE].

[89] CEPC Study Group collaboration, *CEPC conceptual design report: volume 1 — accelerator*, arXiv:1809.00285 [INSPIRE].

[90] ILC collaboration, *The International Linear Collider technical design report — volume 2: physics*, arXiv:1306.6352 [INSPIRE].

[91] LCC Physics Working Group collaboration, *Physics case for the 250 GeV stage of the International Linear Collider*, arXiv:1710.07621 [INSPIRE].

[92] TLEP Design Study Working Group collaboration, *First look at the physics case of TLEP*, *JHEP* **01** (2014) 164 [arXiv:1308.6176] [INSPIRE].

[93] M. He, X.-G. He, C.-K. Huang and G. Li, *Search for a heavy dark photon at future e^+e^- colliders*, *JHEP* **03** (2018) 139 [arXiv:1712.09095] [INSPIRE].

[94] S. Cassel, D.M. Ghilencea and G.G. Ross, *Electroweak and dark matter constraints on a Z' in models with a hidden valley*, *Nucl. Phys.* **B 827** (2010) 256 [arXiv:0903.1118] [INSPIRE].

[95] A. Hook, E. Izaguirre and J.G. Wacker, *Model independent bounds on kinetic mixing*, *Adv. High Energy Phys.* **2011** (2011) 859762 [arXiv:1006.0973] [INSPIRE].

[96] K. Yamamoto, *The phase transition associated with intermediate gauge symmetry breaking in superstring models*, *Phys. Lett.* **B 168** (1986) 341 [INSPIRE].

[97] D.H. Lyth and E.D. Stewart, *Thermal inflation and the moduli problem*, *Phys. Rev.* **D 53** (1996) 1784 [hep-ph/9510204] [INSPIRE].

JHEP03(2019)021